

See discussions, stats, and author profiles for this publication at: <https://www.researchgate.net/publication/226909509>

# BKCa-Channel Structure and Function

CHAPTER · DECEMBER 2006

DOI: 10.1007/0-387-68919-2\_5

---

CITATIONS

5

---

READS

29

## 1 AUTHOR:



Daniel H Cox

Tufts University

28 PUBLICATIONS 1,544 CITATIONS

SEE PROFILE

## 5 BK<sub>Ca</sub>-Channel Structure and Function

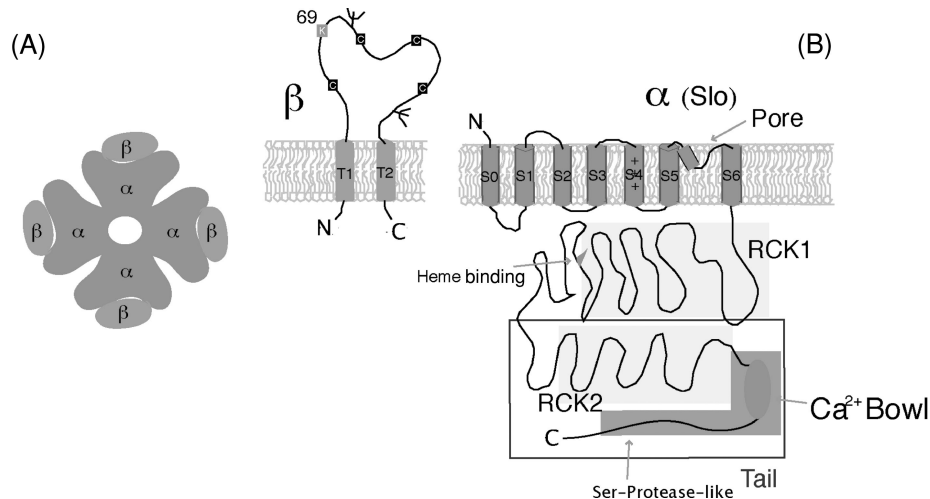
Daniel H. Cox

### 5.1 Introduction

Among ion channels, the large-conductance Ca<sup>2+</sup>-activated K<sup>+</sup> channel (BK<sub>Ca</sub> channel) is in many ways unique. It has a very large single-channel conductance—ten times that of most vertebrate K<sup>+</sup> channels—and yet it maintains strict K<sup>+</sup> selectivity. It senses as little as 200 nM Ca<sup>2+</sup>, but it contains no consensus Ca<sup>2+</sup>-binding motifs, and it is the only channel to be activated by both intracellular Ca<sup>2+</sup> and membrane voltage. In fact, there is a synergy between these stimuli such that the higher the internal Ca<sup>2+</sup> concentration ([Ca<sup>2+</sup>]), the smaller the depolarization needed to activate the channel. Furthermore, the BK<sub>Ca</sub> channel has its own brand of auxiliary subunits that profoundly affect gating. In this chapter, I will discuss what is understood about the origins of these properties in terms of allosteric models and channel structure. At the outset, however, I should say that there is not yet a crystal structure of the BK<sub>Ca</sub> channel or any of its components, so much of the current thinking about BK<sub>Ca</sub>-channel structure relies on analogy to other channels.

### 5.2 BK<sub>Ca</sub>-Channel Topology

BK<sub>Ca</sub> channels are formed by pore-forming  $\alpha$  subunits and in some tissues auxiliary  $\beta$  subunits. Both are integral membrane proteins. Four  $\alpha$  subunits alone form a fully functional channel (Adelman et al., 1992; Shen et al., 1994), while  $\beta$  subunits play a modulatory role (McManus et al., 1995; Orio et al., 2002; Fig. 5.1A). cDNAs encoding a BK<sub>Ca</sub>-channel  $\alpha$  subunit were first identified as the drosophila mutant slowpoke (*slo*) (Atkinson et al., 1991; Adelman et al., 1992). Taking advantage of sequence homologies, *slo* cDNAs were then cloned from many species including human (Butler et al., 1993; Knaus et al., 1994a; Pallanck and Ganetzky 1994; Tseng-Crank et al., 1994; McCobb et al., 1995), and three *slo*-related genes were found. None, however, encode for a Ca<sup>2+</sup>-activated channel—*slo2.1* (Bhattacharjee et al., 2003) and *slo2.2* (Yuan et al., 2000) encode for Na-activated K<sup>+</sup> channels, and *slo3* (Schreiber et al., 1998) encodes for a pH-sensitive K<sup>+</sup> channel. Thus, the original *slo* gene, now termed *slo 1*, *KCNMA1*, or *K<sub>Ca</sub> 1.1*, is the only BK<sub>Ca</sub>-channel gene, and ignoring splice variation mammalian Slo1 proteins share greater than 95% amino acid identity. This strikingly high degree of homology suggests that there has been strong evolutionary pressure to maintain the functioning of these channels within

**Daniel H. Cox**

**Fig. 5.1**  $\text{BK}_{\text{Ca}}$  channels are composed of  $\alpha$  and  $\beta$  subunits. (A) Schematic diagram of a  $\text{BK}_{\text{Ca}}$  channel viewed from the top down. The channel contains four  $\alpha$  and four  $\beta$  subunits. (B) Putative membrane topologies of the  $\text{BK}_{\text{Ca}}\alpha$  and  $\beta$  subunits.

narrow tolerances. Mammalian Slo1 channels are blocked by the classic  $\text{BK}_{\text{Ca}}$ -channel blockers charybdotoxin, iberiotoxin, and tetraethylammonium (Butler et al., 1993; Dworetzky et al., 1996).

Shown in Fig. 5.1B are the proposed membrane topologies of the  $\text{BK}_{\text{Ca}}\alpha$  and  $\beta$  subunits. The  $\alpha$  subunit ( $\sim 1200$  amino acids) is arranged much like a purely voltage-gated ( $K_v$ -type)  $\text{K}^+$  channel subunit, complete with an amphipathic S4 helix that likely forms the channel's voltage-sensor (Bezanilla, 2005), and a  $\text{K}^+$ -channel pore sequence (Heginbotham et al., 1992). Different from  $K_v$  channels, however, the Slo1 subunit has an extra transmembrane segment at its N-terminus, termed S0, that places its N-terminus outside the cell. This was demonstrated by Meera et al. (1997) who showed that an antibody applied extracellularly can bind to an epitope placed at the N-terminus of human Slo1(hSlo1), even if cells transfected with hSlo1 are not permeabilized. The purpose of this  $\text{BK}_{\text{Ca}}$ -specific adaptation is not known, but a study of chimeric channels containing portions of drosophila Slo1 (dSlo1) and mouse Slo1 (mSlo1) has implicated S0 as the site where  $\alpha$  and  $\beta$  subunits interact (Wallner et al., 1996). Perhaps allowing for this interaction is S0's primary function.

The Slo1 subunit also contains a large ( $\sim 800$  amino acid) C-terminal extension that constitutes two thirds of its sequence. This extension contains four somewhat hydrophobic segments that were originally thought to be membrane spanning; however, immunohistochemical and in vitro translation experiments have shown them to be intracellular (Meera et al., 1997). For the purposes of discussion Slo1's cytoplasmic domain may be divided into proximal and distal portions, with a region of low conservation across species marking the division (Butler et al., 1993). It has been argued that the proximal portion contains a domain found in bacterial  $\text{K}^+$  channels

## 5. BK<sub>Ca</sub>-Channel Structure and Function

and transporters termed an RCK domain (Jiang et al., 2001). The distal portion, also known as the “tail”, contains perhaps another RCK domain (Jiang et al., 2002) and a domain that very likely forms a Ca<sup>2+</sup>-binding site termed the “Ca<sup>2+</sup> bowl” (Schreiber and Salkoff, 1997; Bian et al., 2001; Bao et al., 2002, 2004; Niu et al., 2002; Xia et al., 2002). I will discuss the RCK and Ca<sup>2+</sup> bowl domains later, in the context of Ca<sup>2+</sup>-sensing.

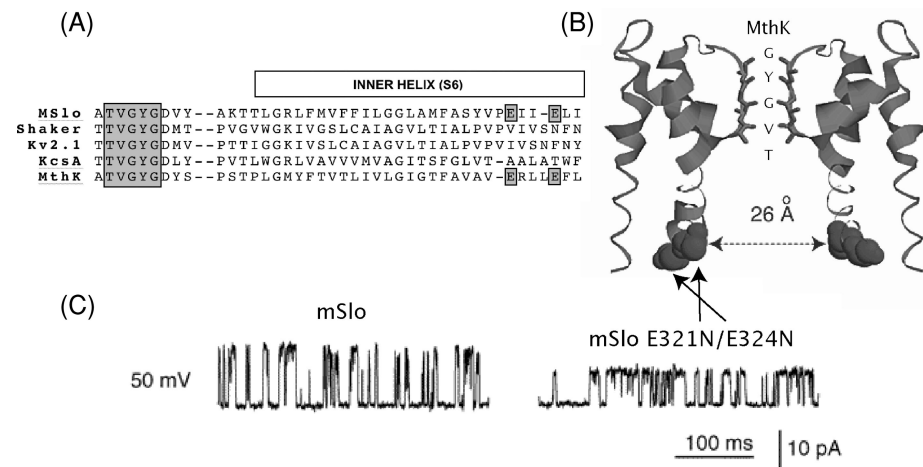
The Slo1 subunit also has a region that binds heme, and nanomolar heme dramatically inhibits channel opening (Tang et al., 2003). The physiological significance of this interaction, however, has yet to be established. Nor in fact has the significance of the observation that part of Slo1’s tail domain has homology to serine proteases (Moss et al., 1996). Both of these regions are indicated in Fig. 1B.

BK<sub>Ca</sub> β subunits (there are now 4) are much smaller than the α subunit (191–279 amino acids). They have two membrane-spanning domains, intracellular N and C termini, and a fairly large extracellular loop (116–128 amino acids) (Knaus et al., 1994a; Lu et al., 2006). This loop contains four cysteine residues that form two disulfide bridges, the pairings of which are unclear (Hanner et al., 1998), and in β 1 a lysine residue (K69) which crosslinks to the external pore-blocker charybdotoxin (Manujos et al., 1995). Four β subunits can interact with a single BK<sub>Ca</sub> channel (Wang et al., 2002). BK<sub>Ca</sub> β subunits will be discussed again later in the context of their functional effects.

### 5.3 The Origin of the BK<sub>Ca</sub> Channel’s Large Conductance

The most striking property of the BK<sub>Ca</sub> channel is its very large single-channel conductance. In symmetrical 150 mM K<sup>+</sup> the BK<sub>Ca</sub> channel has a conductance of 290 pS (Cox et al., 1997a), while other vertebrate K<sup>+</sup> channels have conductances ranging from 2 to 50 pS (Hille, 1992). The prototypical Shaker K<sup>+</sup> channel, for example, has a conductance of 25 pS under these conditions (Heginbotham and MacKinnon, 1993), which means at +50 mV it passes 7.8 million ions per second, while the BK<sub>Ca</sub> channel passes 11.6 times more, or 90 million ions per second. Interestingly, however, the BK<sub>Ca</sub> channel is not less selective for K<sup>+</sup> than Shaker. For every 100 K<sup>+</sup> ions allowed to pass through either channel fewer than 1 Na<sup>+</sup> ion is allowed to pass (Blatz and Magleby, 1984; Yellen, 1984; Heginbotham and MacKinnon, 1993). How is it that the BK<sub>Ca</sub> channel can maintain this high degree of selectivity and yet pass ions much more quickly than other K<sup>+</sup> channels?

A priori one might suppose that it has to do with the structure of the selectivity filter, the narrowest part of the pore, which interacts most closely with the permeating K<sup>+</sup> ions and therefore might reasonably be rate limiting. Crystal structures, however, have been determined now for five K<sup>+</sup> channels: KcsA (Doyle et al., 1998), KvAP (Jiang et al., 2003), MthK (Jiang et al., 2002), KirBac1.1 (Kuo et al., 2003), and Kv1.2 (Long et al., 2005), and despite varying conductances, the selectivity filters of these channels are identical. Each spans about a third of the way

**Daniel H. Cox**

**Fig. 5.2** Rings of negative charge increase the  $\text{BK}_{\text{Ca}}$  channel's conductance. (A) Pore sequences of four  $\text{K}^+$  channels. All four have the  $\text{K}^+$ -channel signature sequence indicated in grey, and mSlo and MthK have two acidic glutamates near the end of S6 shown also in grey. (B) Ribbon diagram of the crystal structure of the pore region of MthK. Indicated in red are the glutamates highlighted in A. (C) Unitary currents from a wild-type mSlo1 channel and a mSlo1 channel that contains the double mutation E321N/E324N. The size of the channel's unitary current is reduced by half by the mutations. The figures in A, B, C, were adapted from Nimigean et al. (2003).

through the bilayer starting from the outside, and the same “signature sequence” TVGYG (Heginbotham et al., 1992) provides carbonyl oxygens that form four  $\text{K}^+$  binding sites (Fig. 5.2A and B).  $\text{K}^+$  ions pass through this filter in single file separated by water molecules (MacKinnon, 2003). The  $\text{BK}_{\text{Ca}}$  channel also contains the “TVGYG” signature sequence, and so does the Shaker channel, so it seems unlikely that it is differences in this structure that account for the  $\text{BK}_{\text{Ca}}$  channel’s unusually large conductance. Similarly, all the crystallized  $\text{K}^+$  channels have wide shallow external mouths that one would suppose would provide good diffusional access to ions entering from the outside (Fig. 5.2B). Indeed, both the  $\text{BK}_{\text{Ca}}$  channel and the Shaker channel (after a point mutation is made) can be blocked from the outside by the pore-plugging toxin charybdotoxin (MacKinnon and Miller, 1988; MacKinnon et al., 1990; Goldstein and Miller, 1992; Stocker and Miller, 1994), which makes specific contacts with the external mouth, so both channels must have similar external architectures.

Given these observations it seems likely that the large conductance of the  $\text{BK}_{\text{Ca}}$  channel arises from modifications inside the channel, on the cytoplasmic side of the selectivity filter. Recent experiments support this notion, and two mechanisms appear to be at play. First, using the crystal structure of the open MthK channel as a guide (Fig. 5.2B; Jiang et al., 2002), it appears that the  $\text{BK}_{\text{Ca}}$  channel has two rings of negatively charged glutamate residues on the inner pore-helix, just at the internal entrance of the channel, and Nimigean et al. (2003) and Breliidze et al. (2003) have shown that when these residues are neutralized to glutamine, the outward

## 5. BK<sub>Ca</sub>-Channel Structure and Function

conductance of the BK<sub>Ca</sub> channel decreases by half (Fig. 5.2C). Thus, part of the reason for the large conductance of the BK<sub>Ca</sub> channel is rings of negative charge at the inner mouth of the channel. These rings attract K<sup>+</sup> creating a ~3.3-fold increase in the local [K<sup>+</sup>]—from 150 mM to 500 mM in the experiments of Breliidze et al. (2003)—and this increases the rate at which K<sup>+</sup> ions encounter the inner mouth of the selectivity filter. In fact, at very high internal [K<sup>+</sup>] (over 1 M) neutralizing these charges has no effect on the channel's conductance (Breliidze et al., 2003) presumably because the local [K<sup>+</sup>] is very high under this condition, even without the negatively charged rings, and the rate of K<sup>+</sup> diffusion to the inner entrance of the selectivity filter is therefore no longer rate limiting (Breliidze et al., 2003).

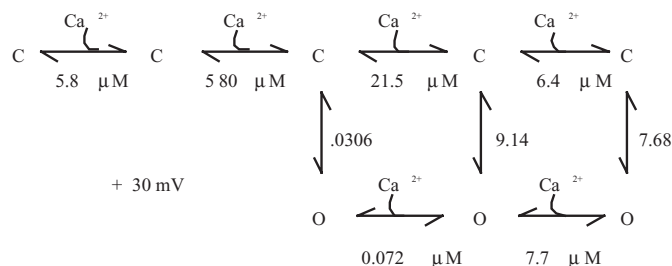
These rings of negative charge, however, must not be the whole story, as their neutralization only reduces the outward K<sup>+</sup> flux by half (at 150 mM K<sup>+</sup> on both side of the membrane) (Breliidze et al., 2003; Nimigean et al., 2003), leaving a channel with still a very large 150 pS conductance. Another mechanism must also be involved, and it seems to be that the internal vestibule and internal mouth are larger in the BK<sub>Ca</sub> channel than they are in other vertebrate K<sup>+</sup> channels. This idea rests on four observations. First, Li and Aldrich (2004) showed that large quaternary ammonium compounds diffuse much more rapidly into the BK<sub>Ca</sub> channel from the inside, on their way to blocking the channel, than they do into the Shaker channel (Li and Aldrich, 2004). Second, once they are inside, the BK<sub>Ca</sub> channel can close behind them, while the Shaker channel cannot (Li and Aldrich, 2004). Third, when Breliidze and Magleby (2005) increased the concentration of sucrose on the internal side of the channel to slow diffusion up to and through the inner vestibule, they found that the BK<sub>Ca</sub> channel's conductance was reduced in a manner that indicated that the rate of motion of K<sup>+</sup> through the inner vestibule is an important determinant of conductance. And four, based on the amount of sucrose needed to make K<sup>+</sup> diffusion from bulk solution to the internal mouth of the channel rate limiting, Breliidze and Magleby (2005) estimated that the BK<sub>Ca</sub> channel's internal mouth is twice as large (20 Å in diameter) as that of the Shaker channel (Webster et al., 2004; Breliidze and Magleby, 2005) and similar in size to the large-conductance (~2004 pS) MthK channel (Jiang et al., 2002) (Fig. 5.2B). Thus, controlling the size and shape of the portion of the pore that is internal to the selectivity filter, and strategically placing charges there to attract K<sup>+</sup> ions, appears to be how nature has produced K<sup>+</sup> channels of differing conductances but common selectivities.

The large conductance of the BK<sub>Ca</sub> channel indicates that the K<sup>+</sup>-channel selectivity filter is exquisitely designed for both selectivity and high throughput, and it suggests that the selectivity filter is not working at maximum capacity in K<sup>+</sup> channels with lower conductances. It is interesting to consider, however, whether as the inner mouth and vestibule of a K<sup>+</sup> channel becomes larger, does more of the membrane potential drop across the selectivity filter. And if so, does the increased electric-field strength drive ions through the selectivity filter more quickly than they can go through in smaller-conductance channels? Perhaps this is another reason for the enhanced conductance of the BK<sub>Ca</sub> channel? As far as I am aware this remains an open question?

Daniel H. Cox

## 5.4 BK<sub>Ca</sub>-Channel Gating, Studies Before Cloning

Because of their large conductance, with the advent of the patch-clamp technique  $\text{BK}_{\text{Ca}}$  channels were among the first channels to be studied at the single channel level, and throughout the 1980s several rigorous studies of their gating behavior were performed (Methfessel, and Boheim, 1982; Magleby and Pallotta, 1983; Moczydlowski, and Latorre 1983; Pallotta, 1983; McManus and Magleby, 1988, 1991; Oberhauser et al., 1988; Latorre et al., 1989; McManus, 1991; Markwardt and Isenberg, 1992). In brief they lead to the following important observations:  $\text{BK}_{\text{Ca}}$  channels can be activated both by  $\text{Ca}^{2+}$  and voltage, and they can be activated by voltage to high open probabilities over a wide range of  $[\text{Ca}^{2+}]$ . Hill coefficients for  $\text{Ca}^{2+}$ -dependent activation are usually observed to be greater than 1 and sometimes as high as 5 (Golowasch et al., 1986). More typically, however, they are between 1 and 4 suggesting that at least four  $\text{Ca}^{2+}$  ions bind to the channel and they act to some degree cooperatively when influencing opening. Analysis of the dwell times of the channel in open and closed states indicates that the channel can occupy at least five closed states and three open states, and that there are multiple paths between closed and open. These observations lead McManus and Magleby in 1991 to propose the following model of  $\text{BK}_{\text{Ca}}$ -channel  $\text{Ca}^{2+}$ -dependent gating at +30 mV.



### Scheme I

Here the channel binds four  $\text{Ca}^{2+}$  ions, and there is a single conformational change between closed and open. Each  $\text{Ca}^{2+}$ -binding step has unique rate constants and therefore also a unique affinity constant (as indicated). After binding the second  $\text{Ca}^{2+}$  ion, the model channel is observed to open with a detectable frequency, but it is the large difference in affinity between the open and closed conformations for the third bound  $\text{Ca}^{2+}$  that drives channel opening. As will be discussed below, although the unique importance of the third binding event is no longer widely accepted, the idea that the channel undergoes a single conformational change allosterically regulated by multiple  $\text{Ca}^{2+}$ -binding events remains an important part of all current models of  $\text{BK}_{\text{Ca}}$ -channel gating.

## 5. BK<sub>Ca</sub>-Channel Structure and Function

### 5.5 BK<sub>Ca</sub>-Channel Gating, Macroscopic Current Properties

The cloning of *slo1* made it possible to express BK<sub>Ca</sub> channels at high density in heterologous expression systems and to study their behavior as a population. Shown in Fig. 5.3A are mSlo1 macroscopic currents recorded from an excised inside-out patch from a *Xenopus* oocyte. The internal face of this patch was exposed to 10 μM Ca<sup>2+</sup>, and the membrane potential was stepped from -80 mV, where the channels were all closed, through a series of increasingly more positive potentials, and then back again to -80 mV. From these data one can determine the conductance of the

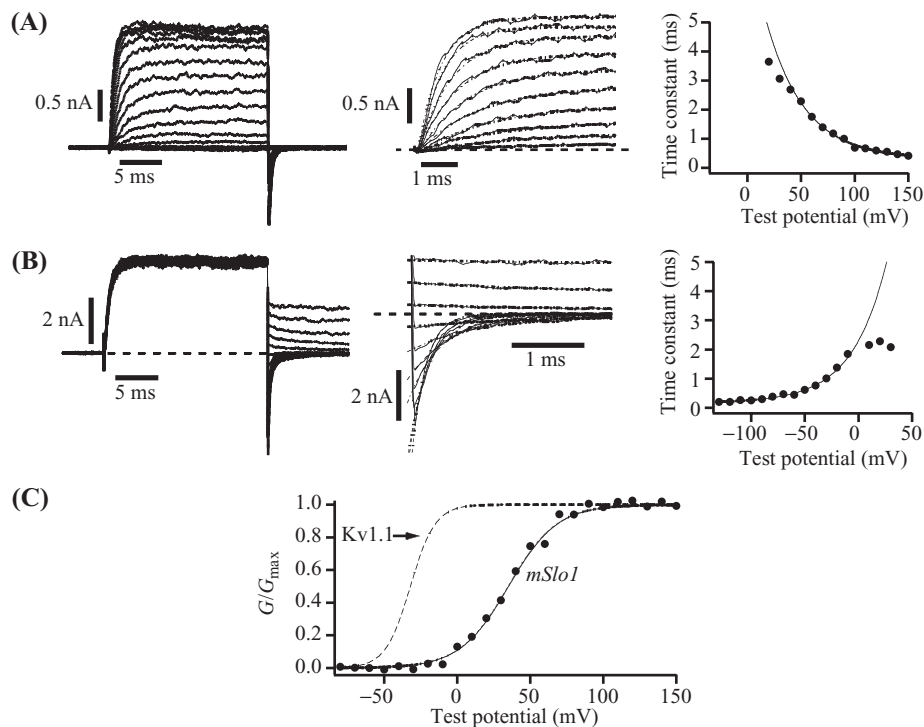


**Figure 5.3** mSlo1 macroscopic currents recorded from *Xenopus* oocyte, inside-out macropatches. The internal face of each patch was exposed to 10 μM [Ca<sup>2+</sup>]. (A) (left) 20 ms pulses from -80 mV to between -80 and +150 mV in 10 mV increments. (middle) The traces on the left have been expanded and fitted with exponential functions. (right) Time constants of activation plotted as a function of voltage. (B) (left) Tail currents recorded in response to repolarization to a series of potentials after depolarization to +100 mV. (middle) The traces on the left have been expanded and fitted with exponential functions. (right) Time constants of deactivation plotted as a function of voltage. (C) Normalized conductance vs. voltage curve ( $G-V$  curve) determined from the data in A. The data have been fitted with a Boltzmann function ( $G/G_{\max} = 1/(1 + e^{qF(V_{1/2}-V)/RT})$ ) with  $V_{1/2} = 24.6$ ,  $q = 1.54$ . Also indicated is the  $G-V$  curve of the mammalian Kv1.1 channel (Grissmer et al. (1994)). This figure was adapted from figure 1 of Cui et al. (1997).

## Daniel H. Cox

membrane as a function of voltage (Fig. 5.3C), and the time course of channel activation (Fig. 5.3A). Similarly, by activating the channels with a prepulse to +100 mV and then stepping back to various potentials, the time course of deactivation can be examined (Fig. 5.3B). Plotted in Fig. 5.3C is the conductance of the mSlo1 channel, relative to its maximum ( $G/G_{\max}$ ), as a function of test potential. As is evident the channel is significantly voltage dependent and exhibits an e-fold change in conductance per 16.5 mV. This corresponds to an apparent gating charge of  $\sim 1.54$  e, which is significant but substantially less than that of the prototypical voltage-dependent K<sup>+</sup> channel, Shaker, or its mammalian homologue Kv1.1 (dashed line).

In Fig. 5.3A (center) the traces from the left have been expanded and the activation time courses fitted with single exponentials. The surprising result here is that, over the entire voltage range, the traces appear well fitted by this simple function. Furthermore, the time course of deactivation is also well fitted by a single exponential at a series of potentials (Fig. 5.3B) (DiChiara and Reinhart, 1995; Cui et al., 1997). Given the complex behavior observed at the single channel level, and the eight states in Scheme I, this is a surprise, as in principle a kinetic scheme with eight states will relax with a time course described by seven time constants. Some of these could be small, and some could be similar to one another, so reasonably one might expect to see fewer than seven, but more than one. Even more striking, however, if one performs the same experiments at a variety of [Ca<sup>2+</sup>] (Fig. 5.4), increasing [Ca<sup>2+</sup>] speeds activation (Fig. 5.4A) and slows deactivation (Fig. 5.4B), but single exponential relaxations are still observed throughout. This result suggests that there is a single rate-limiting conformational change that is influenced by voltage and [Ca<sup>2+</sup>] and dominates the kinetics of channel gating over a wide range of conditions (Cui et al., 1997). To be strictly correct, however, I should say that over a wide range of conditions the kinetics of activation follow an exponential time course but for a very brief delay, on the order of 200  $\mu$ s (Cui et al., 1997; Stefani et al., 1997; Horrigan et al., 1999). The significance of this delay will be made more apparent below.

If one looks at the effect of [Ca<sup>2+</sup>] on the steady-state gating properties of the mSlo1 channel, one sees that Ca<sup>2+</sup> shifts the mSlo1  $G-V$  curve leftward along the voltage axis, with for the most part little change in shape (Fig. 5.5A). This effect is quite dramatic. The shift starts at  $\sim 100$  nM [Ca<sup>2+</sup>] (Meera et al., 1996; Cox and Aldrich, 2000) and continues at concentrations as high as 10 mM, having shifted by this point over 200 mV ([Ca<sup>2+</sup>] up to only 1000  $\mu$ M are shown). Thus, the mSlo1 channel's response to [Ca<sup>2+</sup>] spans five orders of magnitude, and one might reasonably ask how the channel is able to respond to such a wide range of [Ca<sup>2+</sup>]? And what determines the magnitude of the channel's  $G-V$  shift as a function of [Ca<sup>2+</sup>]? The studies described below address these questions.

If one takes the steady-state data of Fig. 5.5A and turns it on its head, plotting now  $G/G_{\max}$  as a function of [Ca<sup>2+</sup>] at several voltages (Fig. 5.5B), one sees that the apparent affinity of the channel for Ca<sup>2+</sup> ranges from less than 1  $\mu$ M to greater than 300  $\mu$ M and is steeply voltage dependent. Early single-channel work suggested that this behavior arises from voltage-dependent Ca<sup>2+</sup> binding (Moczydlowski and

## 5. BK<sub>Ca</sub>-Channel Structure and Function

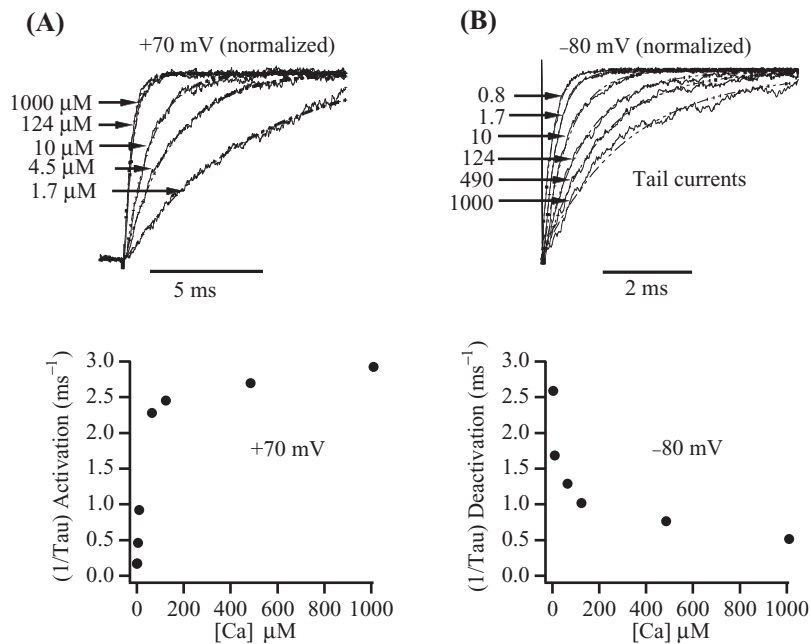


**Figure 5.4** Activation rates increase and deactivation rates decrease with increasing  $[Ca^{2+}]$ . (A) Currents recorded after voltage steps to  $+70$  mV were normalized to their maxima and superimposed. Each curve is fitted with an exponential function, and  $1/\tau$  is plotted in the lower panel as a function  $[Ca^{2+}]$ . (B) Tail currents were recorded at  $-80$  mV, after depolarizations to  $+100$  mV. These currents were then normalized to their minima and superimposed. Each curve is fitted with an exponential function and  $1/\tau$  is plotted as a function of  $[Ca^{2+}]$  in the lower panel. This figure was adapted from figure 6 of Cui et al.(1997).

Latorre, 1983), however, with the cloning of *slo1* it became clear that the Slo1 channel can be near maximally activated in the essential absence of  $Ca^{2+}$  with very strong depolarizations ( $> +300$  mV) (Meera et al., 1996; Cui et al., 1997), and that the rate of channel activation at very low  $[Ca^{2+}]$  is too fast to be due  $Ca^{2+}$ -binding with high affinity after the voltage step (Cui et al., 1997). Thus, the BK<sub>Ca</sub> channel is a voltage-gated channel that is modulated by  $Ca^{2+}$  binding.

## 5.6 A Simple Model of BK<sub>Ca</sub>-Channel Gating

The properties discussed above—a tetrameric channel (Shen et al., 1994), multiple  $Ca^{2+}$  binding sites, a single rate-limiting conformational change between open and closed influenced by both  $Ca^{2+}$  binding and membrane voltage—lead naturally too, and can be accounted for in great part by a simple model of gating known as the voltage-dependent Monnaux Wyman Changeux model, or VD-MWC model (Cui et al., 1997; Cox et al., 1997b). While better and more complex models of BK<sub>Ca</sub>-channel gating exist and will be discussed below, the simplicity and mathematical

### Daniel H. Cox

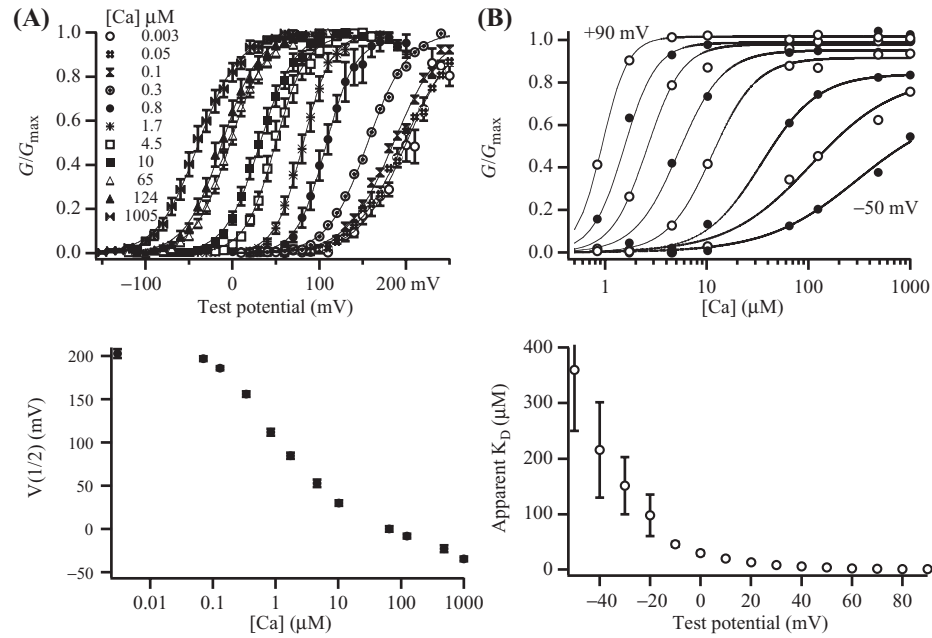
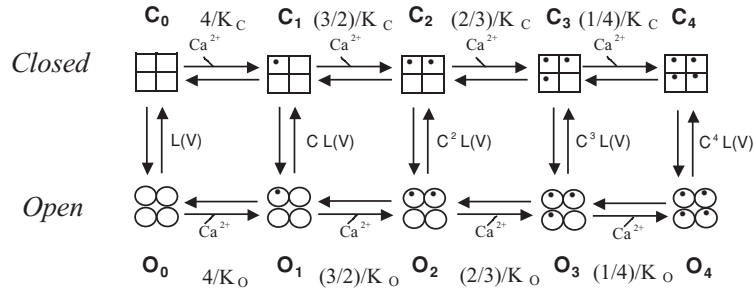


**Figure 5.5** Steady-state gating properties of mSlo1 macroscopic currents as a function of voltage and  $[Ca^{2+}]$ . (A) mSlo1  $G-V$  relations determined at the  $[Ca^{2+}]$  indicated. Each curve has been fitted with a Boltzmann function. In the lower panel  $V_{1/2}$  from the Boltzmann fits is plotted as a function of  $\log[Ca^{2+}]$ . (B) Data like that in A were converted to  $Ca^{2+}$  dose-response curves. The curves displayed were determined at  $-50$  to  $+90$  mV, in 20 mV increments. Each curve has been fitted with the Hill equation (Eq. 5.6), and the  $K_{D-Apparent}$  is plotted as a function of voltage in the lower panel. The figures in A and B, were adapted from Cui et al. (1997).

tractability of the VD-MWC model make it a useful tool by which to gain and intuitive understanding of the properties of an ion channel modulated by both ligand binding and membrane voltage. The VD-MWC model is represented by Scheme II.



Scheme II (The VD-MWC Model)

## 5. BK<sub>Ca</sub>-Channel Structure and Function

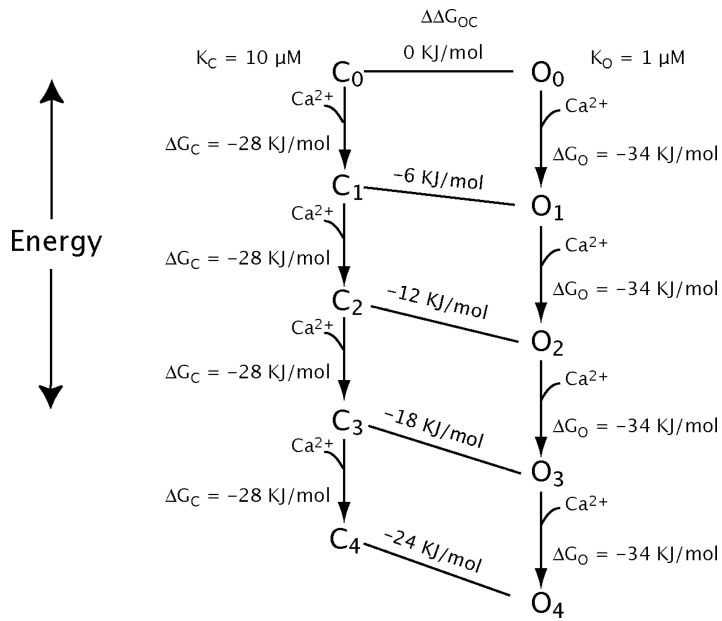
Horizontal steps represent Ca<sup>2+</sup>-binding events, each with dissociation constant  $K_C$  in the closed conformation and  $K_O$  in the open conformation. Vertical steps represent the concerted conformational change by which the channel opens. The equilibrium constant between open and closed in the absence of Ca<sup>2+</sup> is referred to as  $L$ . The MWC model without voltage dependence was first formulated to describe four oxygen molecules binding to homotetrameric hemoglobin (Monod et al., 1965). It is easily adapted to the homotetrameric BK<sub>Ca</sub> channel supposing now four Ca<sup>2+</sup>-binding sites one in each subunit (Cui et al., 1997; Cox et al., 1997b).

Important properties of the MWC model are as follows. In response to ligand-binding individual subunits do not undergo conformational changes on their own, but rather all subunits undergo a conformational change together that is coincident with channel opening. All binding sites are assumed to be identical. The binding of Ca<sup>2+</sup> at one site does not affect the affinities of neighboring sites except indirectly via promoting opening. And, in order for ligand binding to promote opening the open conformation of the channel must bind Ca<sup>2+</sup> more tightly than the closed conformation. We may rely on the law of detailed balance (which does apply to the BK<sub>Ca</sub> channel; McManus and Magleby, 1989) to see why this is so. This law states that for any cyclic gating scheme the product of equilibrium constants on any path between two given states must be equivalent. Considering then the paths between states  $C_0$  and  $O_1$  in Scheme II, we may write

$$\frac{4[\text{Ca}]}{K_C} X = L \frac{4[\text{Ca}]}{K_O}, \text{ which can be rearranged to } X = L \frac{K_C}{K_O}, \quad (5.1)$$

where  $X$  is the equilibrium constant between  $C_1$  and  $O_1$ . Thus, in the MWC model each ligand-binding event alters the equilibrium constant between closed and open by a factor  $C = K_C/K_O$ , a situation with two interesting consequences. First, if  $K_C = K_O$ , Ca<sup>2+</sup> binding will occur, but it will not produce opening, and second, the effect that Ca<sup>2+</sup> binding has on channel opening can be increased by either decreasing  $K_O$ , that is making the open channel bind Ca<sup>2+</sup> more tightly, or increasing  $K_C$ , making the closed channel bind Ca<sup>2+</sup> more weakly. The apparent affinity of the channel, therefore, can increase as a result of a true decrease in binding affinity, a result that demonstrates that even the simplest of ligand-dependent gating systems can behave counter intuitively.

The behavior of the MWC model can be made more intuitive by considering the effect of each binding event in energetic terms. Shown in Fig. 5.6 is the MWC model plotted as an energy diagram, with energy on the vertical. Here  $K_C$  was assumed to be 10 μM and  $K_O$  1 μM, and for simplicity  $L$  was assumed to be 1 such that the energies of the closed and open conformations of the channel are equal in the absence of bound Ca<sup>2+</sup>. Each Ca<sup>2+</sup>-binding event then reduces the energy of the closed channel by  $\Delta G_C = RT \ln K_C$ , or  $-28.3 \text{ KJ mol}^{-1}$ , and it reduces the energy of the open channel by  $\Delta G_O = RT \ln K_O$ , or  $-34.0 \text{ KJ mol}^{-1}$ , such that each Ca<sup>2+</sup>-binding event tips the energetic balance toward opening by  $-5.7 \text{ KJ mol}^{-1}$ . Thus,

**Daniel H. Cox**

**Figure 5.6** Energy diagram for the MWC model. As each  $\text{Ca}^{2+}$  ion binds, the energy of the open and closed conformations are lowered by differing amounts due to differences in binding affinity. This lowers the energy of the open channel relative to the closed. For simplicity  $L$  has been assumed here to equal 1 such that  $C_0$  and  $O_0$  have the same energy. This is not the case for the  $\text{BK}_{\text{Ca}}$  channel where  $L(0)$  is  $\sim 0.0006$ .

it is necessarily the difference between  $\Delta G_O$  and  $\Delta G_C$ , and therefore the ratio of  $K_C$  to  $K_O$ , that drives opening, not their absolute values, and the more  $\text{Ca}^{2+}$ -binding sites the channel has the stronger the effect.

In the VD-MWC model voltage dependence is added simply by supposing that the central conformational change involves the movement of some gating charge  $Q$  through the membrane's electric field such that the equilibrium constant between closed and open becomes voltage dependent. That is

$$L(V) = \frac{[O_0]}{[C_0]} = L(0)e^{\frac{QFV}{RT}}, \quad (5.2)$$

and with this stipulation the open probability of the model is given by

$$P_{\text{open}} = \frac{1}{1 + \left[ \frac{1 + \frac{[Ca]}{K_c}}{1 + \frac{[Ca]}{K_o}} \right]^4 \frac{1}{L(0)} e^{-\frac{QFV}{RT}}}. \quad (5.3)$$

## 5. BK<sub>Ca</sub>-Channel Structure and Function

Even without fitting the data it is apparent by inspection that Eq. 5.3 will display many properties of the BK<sub>Ca</sub> channel. It allows the channel to be maximally activated by voltage in the absence of Ca<sup>2+</sup>, and it has the form

$$P_{\text{open}} = \frac{1}{1 + Ae^{-QFV/RT}}, \quad (5.4)$$

which is a Boltzmann function, with the parameter  $A$  being related to the free energy difference between open and closed in the absence of an applied voltage. For a given  $Q$ , this parameter determines the position of the  $G$ – $V$  curve along the voltage axis, while  $Q$  determines its steepness. In the VD-MWC model  $A$  is Ca<sup>2+</sup> dependent.

$$A = \left[ \frac{1 + \frac{[\text{Ca}]}{K_C}}{1 + \frac{[\text{Ca}]}{K_O}} \right]^4 \frac{1}{L(0)}. \quad (5.5)$$

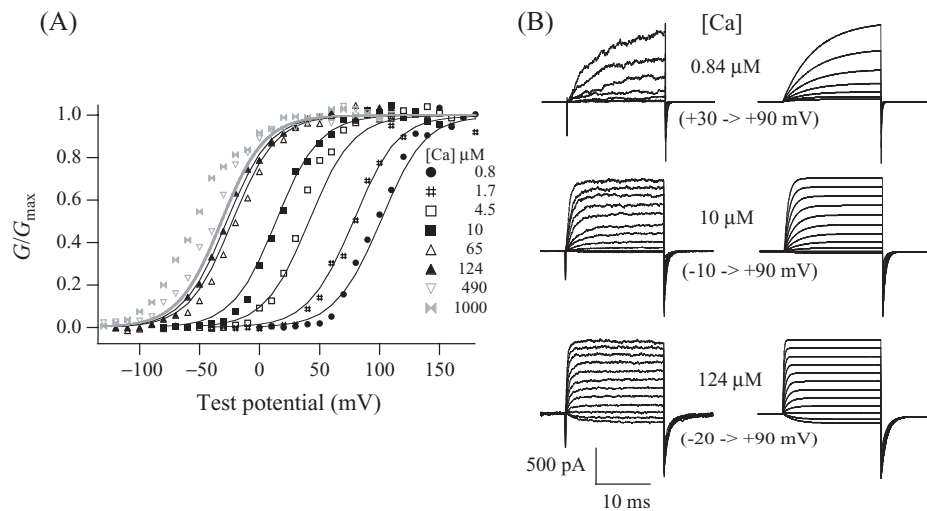
As [Ca<sup>2+</sup>] increases,  $A$  decreases, and the model's  $G$ – $V$  relation shifts leftward along the voltage axis. Since  $Q$  is independent of [Ca<sup>2+</sup>], the model's  $G$ – $V$  relation will not change shape as [Ca<sup>2+</sup>] is varied—it will simply slide along the axis. While this is not true for the BK<sub>Ca</sub> channel, it is true to a first approximation, particularly in the middle [Ca<sup>2+</sup>] range (1–100 μM).

In Fig. 5.7A, a series of mSlo1  $G$ – $V$  curves have been fitted simultaneously with Eq. 5.3, and although the fit is not exceptional, as we expected, the model does a reasonable job of capturing the Ca<sup>2+</sup>-dependent shifting of the mSlo1 channel's  $G$ – $V$  relation. The fit suggests that  $K_C = 11 \mu\text{M}$ ,  $K_O = 1.1 \mu\text{M}$ ,  $L = 0.00061$  and  $Q = 1.40 e$ . Notice, however, that the model is unable to mimic the shifting nature of the mSlo1  $G$ – $V$  curve at [Ca<sup>2+</sup>] greater than 100 μM (data and fits in grey; Cox et al., 1997b). This is now understood to be due the existence of a low-affinity set of Ca<sup>2+</sup>-binding sites that are separate from the channel's higher affinity sites and not included in the model (Shi and Cui, 2001; Zhang et al., 2001).

In Fig. 5.8A and B is shown a series of Ca<sup>2+</sup> dose–response curves determined at different voltages for the mSlo1 channel (*filled*) and the VD-MWC model channel (*open*). Each curve has been fitted with the Hill equation

$$\frac{G}{G_{\max}} = \left[ \frac{\text{Amp}}{1 + \left( \frac{K_D}{[\text{Ca}]} \right)^H} \right], \quad (5.6)$$

and the resulting parameters are plotted in Fig. 5.8C–E. As expected from Fig 5.7,

**Daniel H. Cox**

**Figure 5.7** The VD-MWC model mimics mSlo1 gating. (A) mSlo1  $G$ - $V$  relations fitted with the VD-MWC model (solid lines). All curves were fit simultaneously.  $[Ca^{2+}]$  are as indicated.  $[Ca^{2+}]$  above 124  $\mu M$  are shown in grey and were not included in the fitting. (B) Current families recorded at 0.84  $\mu M$ , 10  $\mu M$ , and 124  $\mu M$  as indicated are shown on the left. VD-MWC-model currents for the same  $[Ca^{2+}]$  are shown on the right. For model parameters see text and Cox et al. (1997b). This figure was adapted from Cox et al. (1997b).

here too the model in many ways recapitulates the data. First, in both the data and the model the extent of activation by  $Ca^{2+}$  is limited by voltage (Fig. 5.8C), second, the Hill coefficient ( $H$ ) is  $\sim 1.5$  to 2 for both the model and the channel over a fairly wide voltage range (Fig. 5.8D), and, three, although the fit is not good at low voltages, the model does predict, as appears in the data, an increase in the channel's apparent  $Ca^{2+}$  affinity (a decrease in  $K_D$ -apparent) as voltage is increased (Fig. 5.8E). Indeed, this occurs even though neither of the model's  $Ca^{2+}$ -binding constants  $K_C$  and  $K_O$  are voltage dependent.

Why is the apparent  $Ca^{2+}$  affinity of the VD-MWC model voltage-dependent even though its binding constants are not? One way to get at this question is to plot open probability ( $P_{\text{open}}$ ) for the model versus the mean number of  $Ca^{2+}$  ions bound (Fig. 5.8F). Such a plot makes it clear that the model becomes more  $Ca^{2+}$  sensitive as voltage is increased, not because it binds  $Ca^{2+}$  more tightly, but because the mean number of bound  $Ca^{2+}$  ions needed to activate the channel becomes smaller. At +160 mV, for example, it takes only 1 bound  $Ca^{2+}$  to activate the channel to a  $P_{\text{open}}$  greater than 0.8, while at 0 mV, 4 bound  $Ca^{2+}$  are required. This is a graphical demonstration of the additive nature of the energies imparted to the closed-to-open conformational change by  $Ca^{2+}$  binding and membrane voltage. For the VD-MWC model  $P_{\text{open}}$  is related to the free energy difference between open and closed,  $\Delta G$ ,

## 5. BK<sub>Ca</sub>-Channel Structure and Function

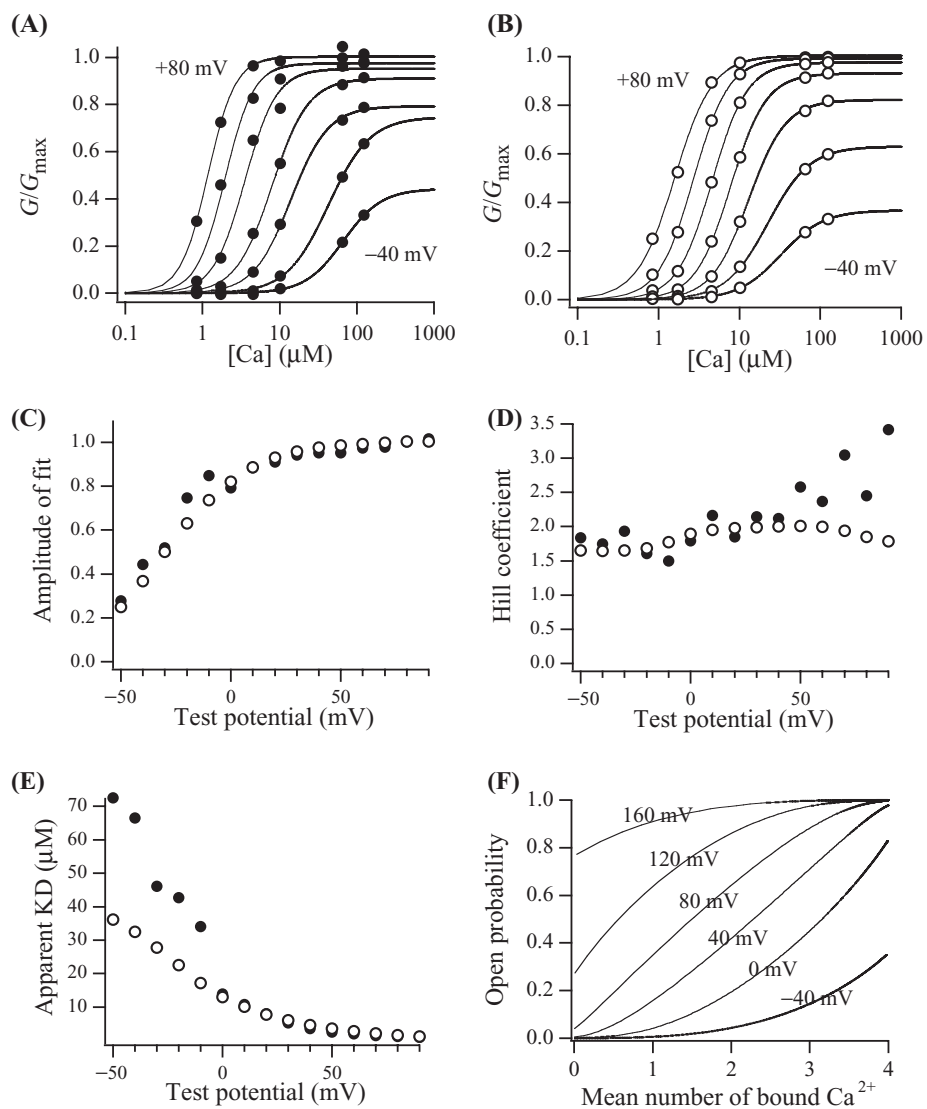


**Figure 5.8** The VD-MWC model mimics the mSlo1 channel's Ca<sup>2+</sup> dose-response curves. (A) Ca<sup>2+</sup> dose-response curves are plotted for seven different voltages ranging from -40 to +80 mV in 20 mV steps (symbols). Each curve is fitted with the Hill equation (Eq. 5.6) (solid curves), and the parameters of these fits are plotted as a function of voltage in C–E. (B) Simulated data from the VD-MWC model. The parameters used for these simulations are those listed in the text. (C–E) Comparison of the fit parameters from the data (closed circles) and the model (open circles). (F) Plots of open probability of the model channel as a function of the mean number of Ca<sup>2+</sup> ions bound to the model channel at a series of voltages. This figure was adapted from those in Cox et al. (1997b).

### Daniel H. Cox

by the following function

$$P_{\text{open}} = \frac{1}{\left(\frac{\Delta G}{RT}\right)} = \frac{1}{\left(\frac{\Delta G_{\text{int rinsic}}}{RT} + \frac{\Delta G_{\text{voltage}}}{RT} + \frac{\Delta G_{\text{Ca}}}{RT}\right)}$$

where

$$\Delta G_{\text{int rinsic}} = -RT \ln(L(0)), \quad (5.7)$$

$$\Delta G_{\text{voltage}} = -QFV/RT,$$

$$\Delta G_{\text{Ca}} = -4RT \ln \left[ \frac{1 + \frac{[\text{Ca}]}{K_O}}{1 + \frac{[\text{Ca}]}{K_C}} \right].$$

Thus, as more energy is supplied for opening by voltage, less is required from  $\text{Ca}^{2+}$ -binding to achieve a given  $P_{\text{open}}$ . This is of course not just true for the VD-MWC model but for a large class of models in which two stimuli are regulating a central conformational change, and it is true for the more complex models to be discussed below.

One might reasonably ask, however, just how far can this go? Can an ion channel have an apparent affinity for its ligand that is higher than the true affinity of any of its binding sites in either conformation? Remarkably, the answer to this question is yes. This is illustrated in Fig. 5.9 where plotted for the model channel is  $P_{\text{open}}$  as a function of  $[\text{Ca}^{2+}]$  at different values of  $L$  ( $K_C = 10$ ,  $K_O = 1$ ) (Fig. 5.9A). These curves were then normalized to have the same maximum and minimum, so that their shapes could be easily compared (Fig. 5.9B), and then the  $[\text{Ca}^{2+}]$  at which the normalized curves are at half of their maximum value is plotted as a function of  $L$  in Fig. 5.9C. At  $L = 1$  the model's  $K_D$ -apparent is  $0.37 \mu\text{M}$  while  $K_O$  is  $1 \mu\text{M}$ . Thus, at even moderate values of  $L$  the apparent  $K_D$  of the model can be smaller than the true  $K_D$  of the open channel. If one repeats this exercise, however, for a channel with only one binding site, one finds that  $K_D$ -apparent cannot be less than  $K_O$ , and it moves from  $K_C$ , when  $L$  is very small, to  $K_O$ , when  $L$  is very large. The peculiar situation, then, where an MWC system displays an apparent affinity higher than any of its real affinities, results from the condition where significantly fewer ligands need to bind to the channel to maximally activate it, than there are binding sites on the channel. For the  $\text{BK}_{\text{Ca}}$  channel this situation would only pertain at voltages greater than  $+100 \text{ mV}$  and not under physiological conditions.

Another question one might ask about the  $\text{BK}_{\text{Ca}}$  channel is what governs its Hill coefficient ( $H$ )? And how should this coefficient—which is a standard measure of the cooperativity of an allosteric system—vary with voltage? The data in Fig. 5.8D tell us that the channel's Hill coefficient slowly increases with voltage from  $\sim 1.5$  to  $\sim 3.0$ , and for the model channel it displays a fairly constant but wavy pattern around the value 1.7. What determines this value? A well known result for the MWC model is that  $H$  for ligand binding is strongly dependent on  $L$  (Segel, 1993), and

## 5. BK<sub>Ca</sub>-Channel Structure and Function

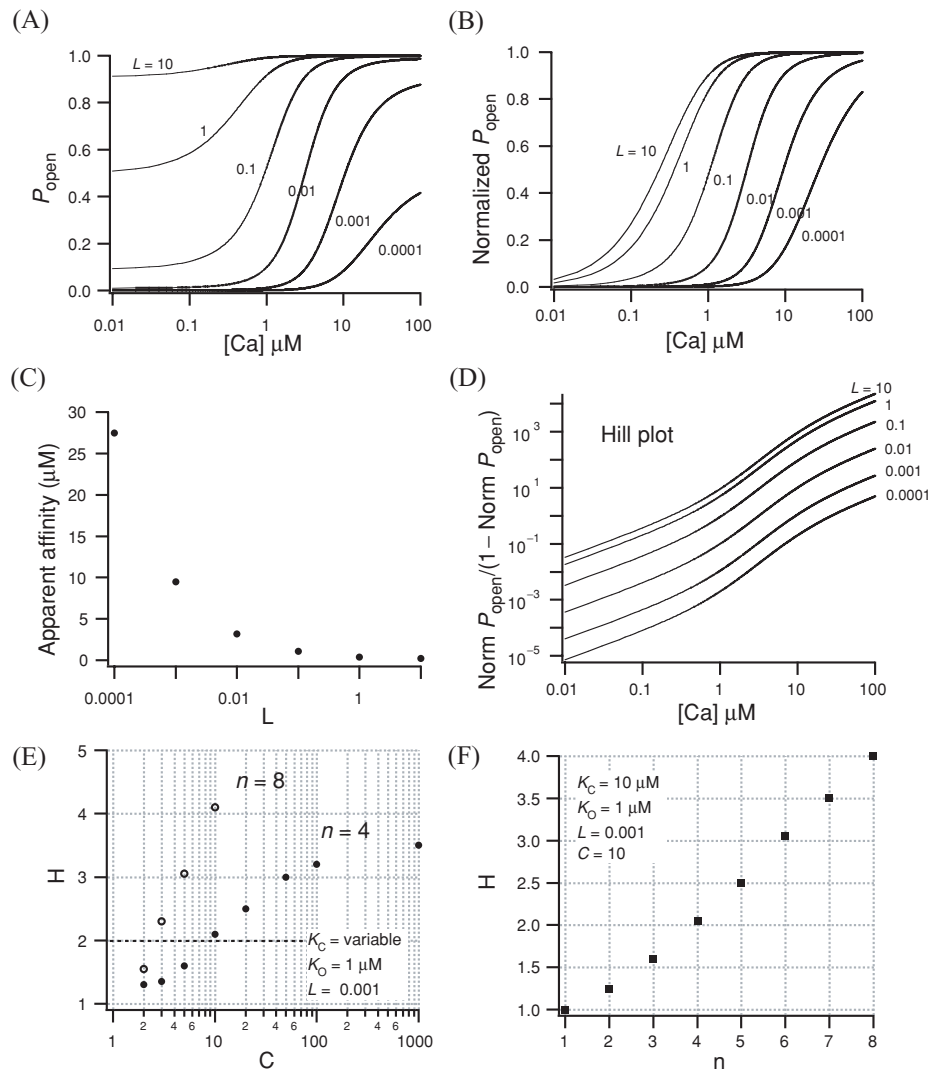


**Figure 5.9** Properties of the MWC model. (A) Simulated dose-response curves for the MWC model where  $K_C = 10$ ,  $K_O = 1$ ,  $n = 4$ , and  $L$  was varied as indicated. (B) The  $0 \text{ Ca}^{2+}$  values of each curve in A were subtracted from each curve, and then they were each normalized to their maximum to yield the curves plotted B. (C) The  $[\text{Ca}^{2+}]$  at which the curves in B are at half of their maximum is plotted as a function of  $L$ . (D) Hill plots for the curves in B. The maximum slope of these relations are defined as the Hill coefficient, which here does not change with  $L$ . (E) Hill coefficient ( $H$ ) plotted as a function of  $C$ , where  $C = K_C/K_O$ . (F) Hill coefficient ( $H$ ) plotted as a function of the number of binding sites  $n$ . Notice  $H$  increases with  $n$  and  $C$ .

## Daniel H. Cox

in the VD-MWC model it is therefore voltage dependent. Interestingly, however, if instead of measuring  $\text{Ca}^{2+}$  binding one measures channel opening,  $H$  for channel opening is independent of  $L$ . This is illustrated in Fig. 5.9D where a series of simulated Hill plots from an MWC model are displayed as a function of  $L$ . Each plot has the same maximum slope and thus the same Hill coefficient. According to this model, then, the  $\text{BK}_{\text{Ca}}$  channel's Hill coefficient should not vary with voltage, and indeed this is true as well for more complex models, so long as voltage sensing and  $\text{Ca}^{2+}$  binding are acting independently on channel opening, and there is only one type of  $\text{Ca}^{2+}$ -binding site.

If this is the case, however, then why does the model's Hill coefficient—and indeed the real channel's—vary in Fig. 5.8D. The answer, at least for the model, is that when the simulated data were fit with the Hill equation, as the voltage was varied, the data were spread over different parts of the  $P_{\text{open}}-V$  curve, and this created an apparent change in  $H$  as different parts of the curve were emphasized in the fitting. However, no real change is expected, and perhaps this technical problem also contributes to the variation in  $H$  observed with fits to the real data. It is now known, however—as will be discussed below—that the  $\text{BK}_{\text{Ca}}$  channel has more than one type of  $\text{Ca}^{2+}$ -binding site, a circumstance that could also give rise to a Hill coefficient that varies with voltage, if different binding sites becomes more or less important for channel opening as the membrane voltage changes.

If  $L$  does not govern the cooperativity of the MWC model, when viewed in terms of channel opening, what does? The answer is  $C$  and  $n$ , where  $n$  represents the number of binding sites the system contains, and again  $C = K_C/K_O$ . Fig 5.9E and F shows that  $H$  increases as  $C$  increases and as  $n$  increases, and that an  $H$  value of  $\sim 2$  for the mSlo1 channel could be explained by supposing that the channel has four binding sites ( $n = 4$ ) with a  $C$  value of  $\sim 10$  ( $C = K_C/K_O$ ), as was done by Cox et al. (1997b), or eight binding sites with a  $C$  value of  $\sim 3$ , which now appears closer to the truth (Bao et al., 2002).

In addition to mimicking many aspects of mSlo1 steady-state gating, the VD-MWC model can also approximate the  $\text{Ca}^{2+}$  and voltage dependence of the kinetics of channel activation and deactivation (Fig. 5.7B) (Cox et al., 1997b). That is, it can be made to activate more quickly with increasing  $[\text{Ca}^{2+}]$  and voltage and deactivate more slowly. To do this rate constants must be supplied for all of the transitions in Scheme II, and two things have been found to be required. (1) The rate constant of channel opening must increase with each  $\text{Ca}^{2+}$ -binding event, while the rate constant for channel closing must decrease, and (2) the on rates and off rates for  $\text{Ca}^{2+}$  binding must be fast. In this limit the VD-MWC model approximates a two state system whose open and closing rates are a weighted average of all the vertical rate constant in Scheme II, each weighted by the percent of closed or open channels that occupy the state that precedes each rate constant (cox et al., 1997b). For the model in Fig 5.7 the  $\text{Ca}^{2+}$  on rates were assumed to be  $10^9 \text{ M}^{-1}\text{s}^{-1}$ , at the very upper end of what is reasonable, and the off rates were then necessarily  $\sim 10^4 \text{ s}^{-1}$  for the closed channel and  $\sim 10^3 \text{ s}^{-1}$  for the open channel. These values produced exponential kinetics under most conditions (Cox et al., 1997b). Thus, many of the

## 5. BK<sub>Ca</sub>-Channel Structure and Function

attributes of both the steady-state and kinetic properties of BK<sub>Ca</sub>-channel gating can be accounted for by the simple VD-MWC scheme, and what it seems to be telling us is that, if there are four independent binding sites, then each has a  $K_C$  of  $\sim 10 \mu\text{M}$  and a  $K_O$  of  $\sim 1 \mu\text{M}$ , and the binding and unbinding of Ca<sup>2+</sup> must be fast.

### 5.7 Interpreting Mutations

A useful aspect of the VD-MWC model and something that is not the case for models with more complicated voltage-sensing mechanisms is that is easy to write down the equation that governs its  $G-V$  position as a function of [Ca<sup>2+</sup>]. Here in terms of the voltage of half-maximal activation  $V_{1/2}$

$$V_{1/2} = \frac{4RT}{QF} \ln \left[ \frac{(1 + [\text{Ca}] / K_C)}{(1 + [\text{Ca}] / K_O)} \right] + \frac{RT}{QF} \ln[L(0)]. \quad (5.8)$$

This equation states that  $V_{1/2}$  in 0 [Ca<sup>2+</sup>] depends on  $L$  and  $Q$ , and the extent to which it moves with increasing [Ca<sup>2+</sup>] depends on  $K_C$ ,  $K_O$ , and  $Q$ . An important result here is that the steepness of the  $V_{1/2}$  vs. [Ca<sup>2+</sup>] relation depends on the channel's Ca<sup>2+</sup> dissociation constants, as one might imagine, but also on  $Q$ . All other things being equal the larger  $Q$  is, the smaller the shift. Thus, if one were to make a mutation that affects the slope of the BK<sub>Ca</sub> channel's  $V_{1/2}$  vs. [Ca<sup>2+</sup>] relation, the VD-MWC model suggests that this could either be due to a change in voltage sensitivity or a change in Ca<sup>2+</sup> binding. We can determine which, however, by rearranging Eq. 5.8 to

$$QFV_{1/2} = 4RT \ln \left[ \frac{(1 + [\text{Ca}] / K_C)}{(1 + [\text{Ca}] / K_O)} \right] + RT \ln[L(0)], \quad (5.9)$$

(where  $-QFV_{1/2}$  is equal to the energy difference between open and closed) and instead of plotting  $V_{1/2}$  vs. [Ca<sup>2+</sup>], plotting  $QFV_{1/2}$  vs. [Ca<sup>2+</sup>]. On such a plot the position of the curve at 0 [Ca<sup>2+</sup>] is determined solely by  $L$ , while the shape of the curve is determined by  $K_C$  and  $K_O$  (Cox et al., 1997b; Cox and Aldrich, 2000; Cui and Aldrich, 2000). The VD-MWC model, therefore, provides a straightforward means by which to distinguish between mutations that effect voltage sensing ( $Q$ ), Ca<sup>2+</sup> binding ( $K_C$  or  $K_O$ ), and the intrinsic energetics of channel opening ( $L(0)$ )).

### 5.8 A Better Model of Voltage-Dependent Gating

Although the VD-MWC model provides a useful framework for thinking about a channel regulated by voltage and ligand binding, there are aspects of the BK<sub>Ca</sub> channel's gating behavior that fails to mimic. It does not predict the brief delay (200 μs) in activation mentioned above. It does not mimic well the kinetic behavior of the channel at far positive and far negative voltages, and it predicts that in the absence

Daniel H. Cox

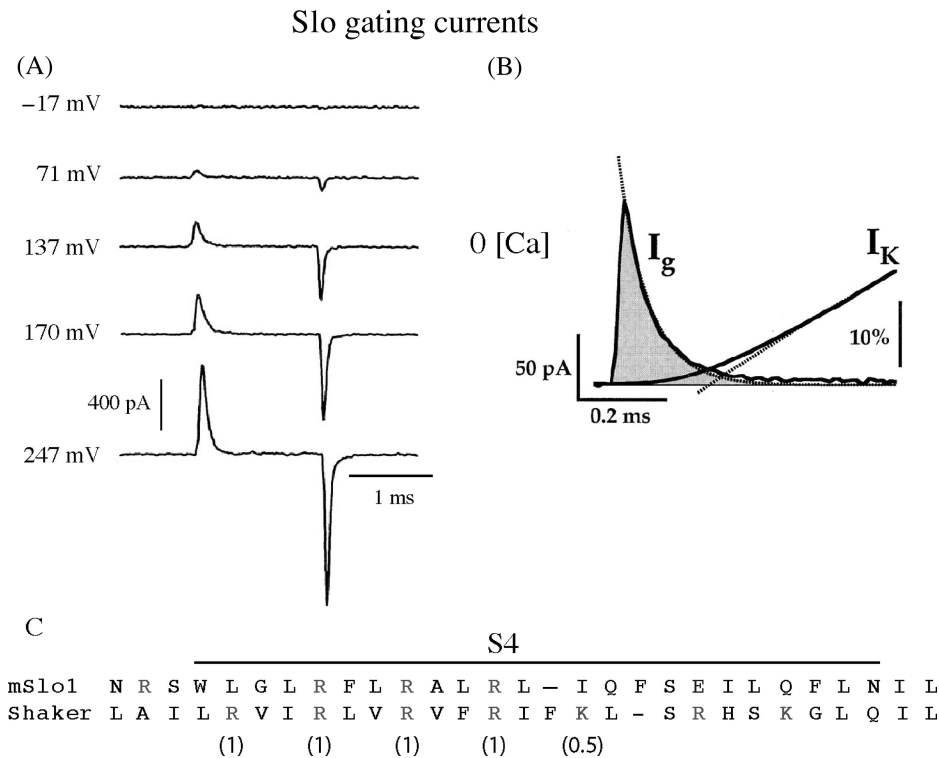


**Figure 5.10** BK<sub>Ca</sub>-channel gating currents are fast. (A) hSlo1 gating currents recorded with pulses to the indicated potentials in the absence of [Ca<sup>2+</sup>]. (B) □□□□ ( $I_g$ ) and the time course of ionic current activation ( $I_K$ ). Gating charge moves before the channels open. (C) Alignment of the S4 regions of the mSlo1 channel and the Shaker channel. Positively charged residues are boxed. Negatively charged residues are circles. A was adapted from Stefani et al. (1997). B was adapted from Horrigan and Aldrich (1999).

Au: Please provide the missing text.

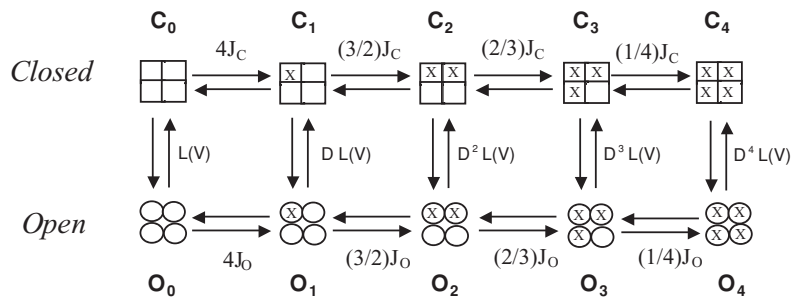
of Ca<sup>2+</sup>, single channel recordings should reveal only a single open state and a single closed state, while the mSlo1 channel displays three closed and two open states under this condition (Talukder and Aldrich, 2000). The most damning evidence against the VD-MWC model, however, is the important observation—initially made by Stefani et al. (1997) (see Fig. 5.10A), and then Horrigan and Aldrich (1999) (see Fig. 5.10B)—that BK<sub>Ca</sub>-channel gating currents are much faster than channel opening and closing (Fig. 5.10B). The VD-MWC model predicts the two processes should have the same time constant, as in the VD-MWC model voltage-sensor movement is part of the central closed-to-open conformational change.

That this is not the case for the BK<sub>Ca</sub> channel, however, perhaps should not be surprising as the Shaker channel's gating currents also relax more quickly than the channel opens, and this has been explained by supposing that voltage sensors in each subunit move rapidly upon depolarization, and when all have moved to their active conformation the channel undergoes an opening conformational change

## 5. BK<sub>Ca</sub>-Channel Structure and Function

(which is also weakly voltage-dependent) (Bezanilla, 2005). Three things about the BK<sub>Ca</sub> channel's gating currents, however, are very different from those of Shaker. BK<sub>Ca</sub>-channel gating currents are much smaller, they are much faster, and their off gating currents are not slowed by channel opening (Stefani et al., 1997; Horrigan and Aldrich, 1999). With Shaker the voltage sensors must wait for the channel to close before they can return to their resting state, while this is not the case for mSlo1 (Zagotta et al., 1994; Bezanilla, 2005).

In 1999, based on an extensive series of both gating and ionic current experiments with the mSlo1 channel, Horrigan, Cui, and Aldrich proposed a model of BK<sub>Ca</sub>-channel voltage-dependent gating that does a remarkably good job of accounting quantitatively for almost all aspects of BK<sub>Ca</sub>-channel gating in the absence of Ca<sup>2+</sup> (Horrigan et al., 1999; Horrigan and Aldrich, 1999). This model, termed here the HCA model, is represented by Scheme III.



$$J_C = e^{\frac{z_J F (V - V_{hc})}{RT}} \quad J_O = e^{\frac{z_J F (V - V_{ho})}{RT}}$$

$$L(V) = L e^{z_L F V / RT} \quad D = \frac{J_O}{J_C}$$

Scheme III

Notice it looks very much like the MWC model except here horizontal transitions represent voltage-sensor activation, now one in each subunit, and the central closed-to-open conformational change is also proposed to weakly voltage dependent. Thus, the HCA model is an allosteric model of voltage-dependent gating, where instead of voltage-sensor movement being required for channel opening, as is the case with the VD-MWC model and models of Shaker gating, here the channel can open with any number of voltage sensor's active, but as each voltage sensor moves to its active state, the open conformation of the channel becomes energetically more favored. Also analogous to the MWC model, in the HCA model, in order for voltage-sensor movement to promote channel opening it must lower the energy of the open state

## Daniel H. Cox

of the channel more than the energy of the closed state. Practically speaking, what this means is the  $V_{1/2}$  for voltage-senor movement must be more negative when the channel is open than when it is closed. Analogous to the factor  $C$  in the MWC model, Horrigan, Cui, and Aldrich defined  $D$  to represent the factor by which the movement of a voltage senor in the HCA model increases the equilibrium constant between open and closed. They estimated  $D$  to be 17 for the mSlo1 channel (Horrigan et al., 1999; Horrigan and Aldrich, 1999).

There are five parameters that govern the equilibrium behavior of the HCA model.  $L(0)$  the equilibrium constant between open and closed at 0 mV when no voltage sensors are active,  $z_q$  the gating charge associated with this equilibrium constant,  $V_{hc}$  and  $V_{ho}$  the half-activation voltages of voltage-sensor movement when the channel is closed or open respectively, and  $z_j$  the gating charge associated with each voltage sensor's movement. By measuring open probabilities at very low voltages, Horrigan et al. (1999) and Horrigan and Aldrich (1999) were able to determine  $L(0)$  to be  $\sim 2 e^{-6}$  and  $z_q$  to be  $0.4 e$ . By measuring gating currents and macroscopic ionic currents over a wide range of voltages, they were able to estimate  $V_{hc}$  to be +155 mV,  $V_{ho}$  to be 24 mV and  $z_j$  to be  $0.55 e$ . With these parameters the HCA model nicely mimics the mSlo1 channel's  $Q$ - $V$  and  $G$ - $V$  curves in the absence of  $\text{Ca}^{2+}$ . Indeed a key feature of the data that is reproduced by the model is that at very low open probabilities the mSlo1  $\log(P_{\text{open}})$ -vs.-voltage relation reaches a limiting slope that is less than the maximum slope of this relation and reflects just the voltage dependence of the central conformational change (Horrigan et al., 1999).

Also, by studying the kinetics of gating and ionic currents Horrigan et al. (1999) and Horrigan and Aldrich (1999) were able to specify all the rate constants in Scheme III and then reproduce very well the kinetic behavior of both gating and ionic currents. In qualitative terms what their work and that of Stefani et al. (1997) suggests is that in response to changes in voltage the channel's voltage sensors move very rapidly and independently between an active and an inactive state, with the process of channel opening and closing being much slower. Indeed, in response to depolarization the voltage sensors of the closed channel reequilibrate completely during the brief delay ( $\sim 200 \mu\text{s}$ ) that precedes macroscopic current activation (see Fig. 5.10B), and then, as the channels open, they equilibrate again among open states. Upon repolarization the voltage sensors equilibrate very rapidly among open states, before the channels close, and then they equilibrate again through the closed states as the channels close. Combining these results, then, with observations from VD-MWC modeling, it appears that the essentially monoexponential nature of the  $\text{BK}_{\text{Ca}}$  channels macroscopic currents arises from a channel whose closed-to-open conformational change is rate limiting under nearly all conditions and is allosterically regulated by the faster processes of  $\text{Ca}^{2+}$  binding and voltage-sensor movement.

Each voltage sensor in the HCA model carries a gating charge of  $0.55 e$ , while each voltage sensor of the Shaker channel carries a gating charge of  $\sim 3.5 e$  (Bezanilla, 2005). Thus the  $\text{BK}_{\text{Ca}}$  channel's voltage sensor appears to carry only 1/6 the gating charge of that of the Shaker channel. For the Shaker channel the gating

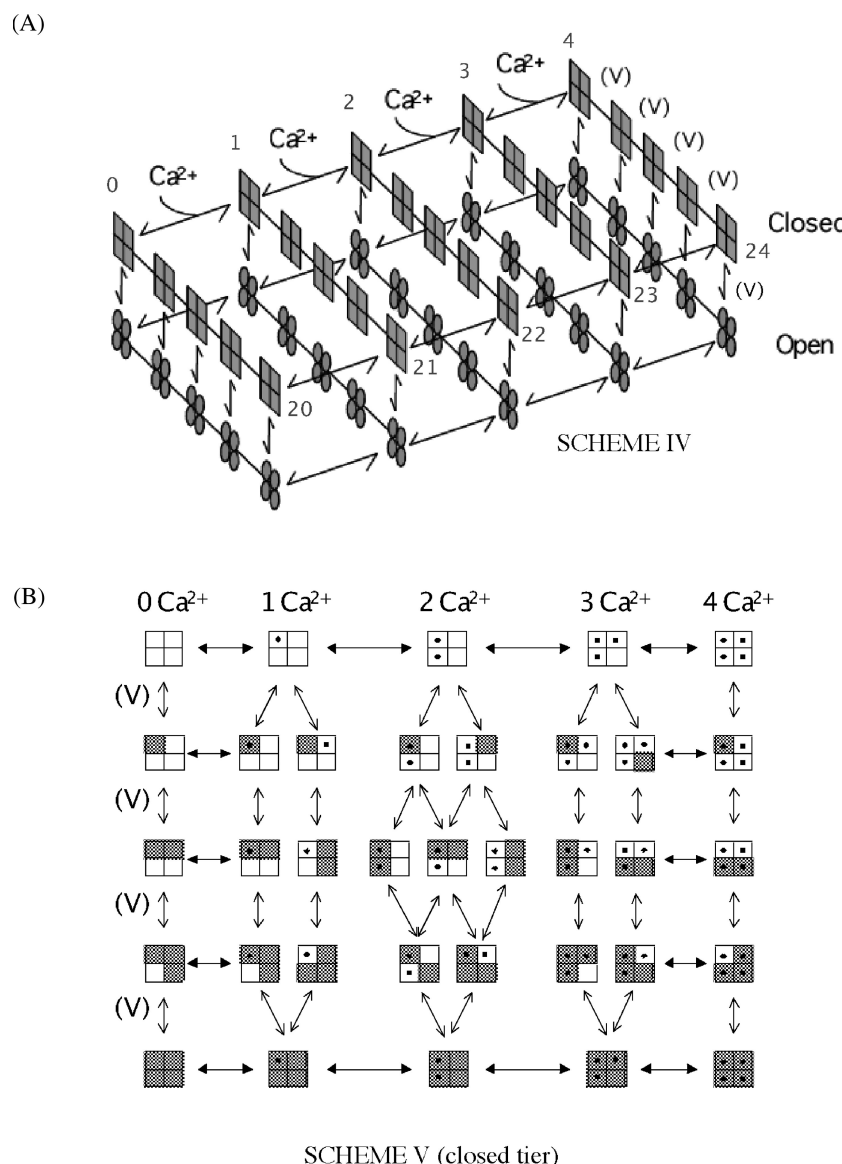
## 5. BK<sub>Ca</sub>-Channel Structure and Function

charge has been shown to arise from the movement of 5 of 7 positively charged residues in the S4 segment (Aggarwal and MacKinnon, 1996; seoh et al. 1996). An alignment of the Shaker and mSlo1 S4 segments is shown in Fig 5.10C. The residues that carry gating charge along with the approximate amount of charge they carry (according to Agarwall and MacKinnon, 1996) are indicated in parentheses. The BK<sub>Ca</sub> channel shares the 2nd, 3rd, and 4th positive charges that in the Shaker channel contribute 1 full charge each to the gating charge. Thus, it is surprising that the BK<sub>Ca</sub> channel's voltage sensor does not contain a larger amount of gating charge, and if this is indeed the case, as it appears to be, then it suggests either that the movements that this region undergoes during gating are not the same for the two channels, or the electrical fields through which these movements occur are very different. Indeed, one might question whether S4 is involved at all in the voltage sensing of the BK<sub>Ca</sub> channel. Mutagenesis experiments, however, suggest that R213 and R210 carry a small amount of gating charge (Diaz et al., 1998), so the S4 segment may form the voltage sensor of both channels, but the reason why R207, R210, and R213 do not contribute more gating charge to mSlo1 remains a mystery.

## 5.9 Combining HCA and MWC

Given the success of MWC-like models in describing Ca<sup>2+</sup> sensing, and the HCA model in describing voltage sensing, it is natural to combine the two to produce a model of BK<sub>Ca</sub>-channel gating-like that shown in Fig. 5.11A. Here the top tier of states represents the closed conformation of the channel, and the bottom tier the open conformation. The horizontal transitions along the long axis represent Ca<sup>2+</sup> binding and unbinding. The horizontal transitions along the short axis represent voltage-sensor movement. There is one open state and one closed state for every possible combination of 1–4 voltage sensors active and 1–4 Ca<sup>2+</sup>-binding sites occupied, and thus 25 closed and 25 open states, or 50 states in all. Rothberg and Magleby (2000) where the first to propose that a model of this form could mimic the essential aspects of the gating of the BK<sub>Ca</sub> channel based on their analysis of the mSlo1 channel's single-channel behavior over a wide range of conditions.

At first glance this 50-state model might seem hopelessly complex, but it is based on simple ideas about Ca<sup>2+</sup> and voltage sensing. And although it has many states, if voltage sensors and Ca<sup>2+</sup>-binding sites are considered identical and independent, its open probability is determined by just seven parameters—the five HCA parameters,  $L(0)$ ,  $z_q$ ,  $V_{hc}$ ,  $V_{ho}$ , and  $z_j$ , plus the MWC parameters  $K_C$  and  $K_O$ —so there is reason to hope that they could be well constrained by electrophysiological data. Indeed, Cox and Aldrich (2000), using voltage-sensing parameters close to those determined from HCA modeling (Horrigan and Aldrich, 1999), and Ca<sup>2+</sup> dissociation constants close to those determined from VD-MWC modeling (Cox et al., 1997b), were able to describe the shifting nature of the mSlo1  $G-V$  relation between 0 and 100 μM [Ca<sup>2+</sup>] fairly well (Cox and Aldrich, 2000).

**Daniel H. Cox**

**Figure 5.11** Allosteric models of  $\text{BK}_{\text{Ca}}$ -channel gating (A) 50-state model first proposed by Rothberg and Magleby (2000). (B) The 35 states of one tier of the 70-state model of Horrigan and Aldrich (2002). A was adapted from Cox and Aldrich (2000). B was adapted from Cox et al. (1997).

## 5. BK<sub>Ca</sub>-Channel Structure and Function

One possibility that the 50-state model ignores, however, is that Ca<sup>2+</sup> binding to its site in a given subunit may directly alter the equilibrium for voltage sensor movement in that same subunit and vice versa. If one takes this possibility into account then the 50-state model must be expanded to a 70-state scheme with now 35 closed and 35 open states (Cox et al., 1997b), and one more parameter  $E$  must be added (Horigan and Aldrich, 2002). Analogous to  $C$  and  $D$ ,  $E$  is the intrasubunit coupling factor between Ca<sup>2+</sup> binding and voltage sensing. The 35 closed states of such a model are depicted graphically in Fig. 5.11B. One has to imagine each of these closed states being connected through an opening conformational change to a corresponding open state. The open probability of the resulting 70-state model, first proposed by Horigan and Aldrich (2002), is given by the following equation

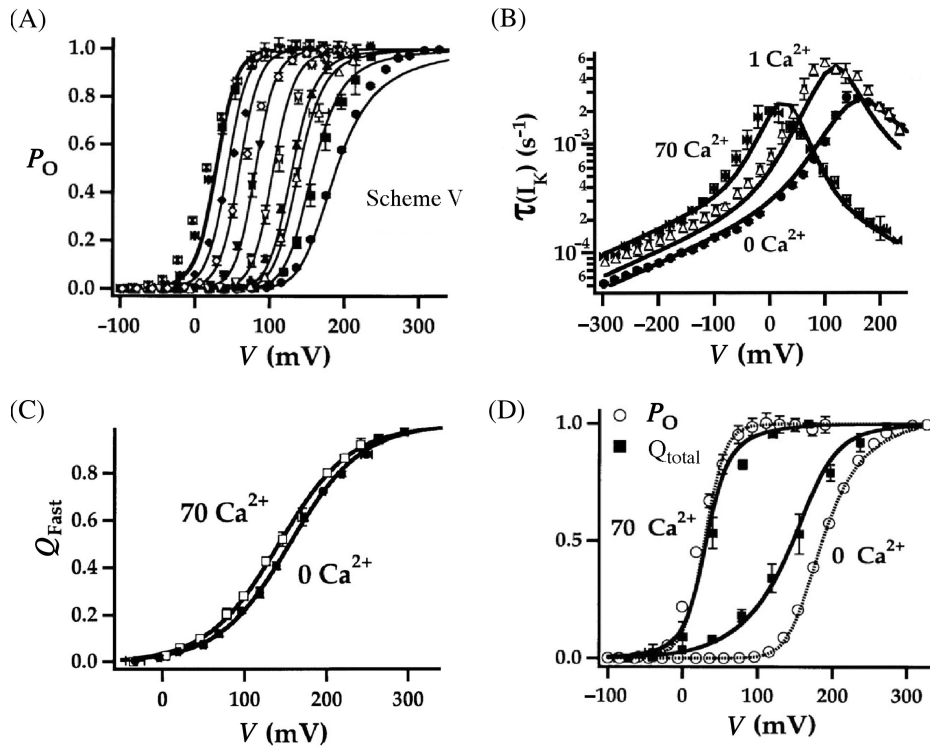
$$P_{\text{open}} = \frac{L(1 + K_O + J_O + J_O K_O E)^4}{L(1 + K_O + J_O + J_O K_O E)^4 + (1 + J_C + K_C + J_C K_C E)^4} \quad (5.10)$$

where

$$\begin{aligned} L &= L(0)e^{\frac{z_F F V}{RT}}; & J_O &= J_O(0)e^{\frac{z_J F(V - V_{ho})}{RT}}; & J_C &= J_C(0)e^{\frac{z_J F(V - V_{hc})}{RT}}; \\ K_C &= \frac{[\text{Ca}]}{K_C}; & K_O &= \frac{[\text{Ca}]}{K_O}. \end{aligned}$$

But are the 20 extra states needed? Does Ca<sup>2+</sup> binding in fact directly affect voltage sensing? Is  $E$  different from 1? Experiments with mutations that alter voltage sensing suggest it is not (Cui and Aldrich, 2000); however, Horigan and Aldrich (2002) addressed this issue directly by measuring mSlo1 gating currents in 0 and 70 μM [Ca<sup>2+</sup>]. They made the following interesting observations. mSlo1 on gating currents exhibit two exponential components, fast and slow.  $Q_{\text{fast}}$  can be assigned to the rapid equilibration of voltage sensors in the closed channel before the channel opens, and  $Q_{\text{slow}}$  to the reequilibration of the voltage sensors among open-states after the channels open. As this second component of charge movement is limited by the speed of channel opening, it appears slow even though, once a channel is open, its voltage sensors reequilibrate rapidly. The interesting result, however, is that, while increasing [Ca<sup>2+</sup>] from 0 to 70 μM has a large effect on the  $Q_{\text{total}}-V$  relation (fast + slow)—it makes this curve much steeper and shifts it to the left (see Fig. 12D)—it has very little effect on the  $Q_{\text{fast}}-V$  relation. It shifts it just –20 mV, and it does not change its shape (Fig. 5.12C). Since this relation reflects the activation of voltage sensors in the closed channel, the fact that it changes little when [Ca<sup>2+</sup>] is increased indicates that indeed Ca<sup>2+</sup> binding does not have a large direct effect on voltage-sensor movement. That is,  $E$  is small. The –20 mV shift, however, does indicate that it is not equal to 1. Horigan and Aldrich estimated it to be 2.4.

If the  $Q_{\text{fast}}-V$  relation does not change much with increasing [Ca<sup>2+</sup>], then why does the  $Q_{\text{total}}-V$  relation change so dramatically with increasing [Ca<sup>2+</sup>] (Fig. 5.12D)? It turns out this is not so strange, and it is predicted by the 70-state

**Daniel H. Cox**

**Figure 5.12** mSlo gating and ionic currents can be well described by the HA model (Scheme V see Fig. 5.11B). (A)  $G$ - $V$  relations determined at the following  $[Ca^{2+}]$ , from right to left in  $\mu M$ : 0.27, 0.58, 0.81, 1.8, 3.8, 8.2, 19, 68, and 99. The curves were simultaneously fit with the HA model (continuous lines) with the following parameters:  $K_C = 11 \mu M$ ,  $K_o = 1.4 \mu M$ ,  $V_{hc} = 150$  mV,  $V_{ho} = 0.7$  mV,  $z_q = 0.4$ ,  $z_J = 0.55$ ,  $L(0) = 2 \times 10^{-6}$ . (B) The HA model can also mimic the kinetic behavior of mSlo1 macroscopic currents. Plotted are macroscopic current relaxation time constants as a function of membrane voltage. Continuous lines represent fits to Scheme V. Steady-state parameters were the same as in A. For kinetic parameters see Horrigan and Aldrich (2002, Table III). (C) There is little change in the  $Q_{fast}$ - $V$  relation of the mSlo1 channel when  $[Ca^{2+}]$  is raised from 0 to 70  $\mu M$ . The small shift observed is  $-20$  mV. (D) The HA model (continuous lines) can also reproduce the changes observed in the relationship between the mSlo1  $Q_{total}$ - $V$  relation and the  $P_{open}$ - $V$  relation as  $[Ca^{2+}]$  is increased. This change occurs because as  $[Ca^{2+}]$  is increased fewer voltage sensors need to move to open the channel. All panels were adapted from figures in Horrigan and Aldrich (2002).

or HA model. For a detailed explanation I refer the reader to the original publication (Horrigan and Aldrich, 2002). In brief, however, the answer is that the  $Q_{total}$ - $V$  relation of the HA model is a weighted average of the  $Q$ - $V$  relations of the open and closed channels—with midpoints  $V_{hc}$  and  $V_{ho}$  respectively—weighted by the fraction of channels that are open and closed at a given voltage. These relations have the same shape but lie  $\sim 140$  mV apart on the voltage axis. The addition of  $Ca^{2+}$  makes the channels open at lower voltages and thereby puts greater weight on

## 5. BK<sub>Ca</sub>-Channel Structure and Function

the  $Q_{\text{open}}-V$  relation than the  $Q_{\text{closed}}-V$  relation. According to the HA model, it is changes in the weighting of these two curves with increasing  $[\text{Ca}^{2+}]$  that cause the large change in shape and position of the  $Q_{\text{total}}-V$  curve.

Notice also in Fig. 5.12D that at 0  $[\text{Ca}^{2+}]$  the  $Q_{\text{total}}-V$  relation lies to the left of the  $\bullet\bullet\bullet V$ , and it is more shallow, while at high  $[\text{Ca}^{2+}]$ , the  $Q_{\text{total}}-V$  relation is very similar in shape and position to the  $P_{\text{open}}-V$  curve. This makes sense, as in 0  $[\text{Ca}^{2+}]$  on average three voltage sensors must become active before the channel opens, while in 70  $\mu\text{M}$   $[\text{Ca}^{2+}]$  just one is required (Horri gan and Aldrich, 2002).

Not only did Horri gan and Aldrich show that their model could explain the behavior of the channel's gating currents, they also found a set of parameters that could fit the channel's  $G-V$  relation with  $[\text{Ca}^{2+}]$  between 0 and 70  $\mu\text{M}$  (Horri gan and Aldrich, 2002) (Fig. 5.12A). Their estimates of  $K_C$  and  $K_O$ , assuming four  $\text{Ca}^{2+}$ -binding sites, were 11  $\mu\text{M}$  and 1.4  $\mu\text{M}$ ,  $C = 8$ , similar to estimates from the VD-MWC model. And they also found rate constants for the closed-to-open transitions in the model that enabled it to reproduce the channel's macroscopic-current kinetics fairly well (Fig. 5.12B). To approximate exponential kinetics again  $\text{Ca}^{2+}$  binding was assumed to be fast. Thus, the HA model reproduces BK<sub>Ca</sub>-channel behavior over an impressively wide range of conditions, and it is the best explanation of BK<sub>Ca</sub>-channel gating to date. Indeed, it also allows for variations in  $G-V$  steepness as a function of  $[\text{Ca}^{2+}]$ , something else observed in the data and not accounted for by the VD-MWC model.

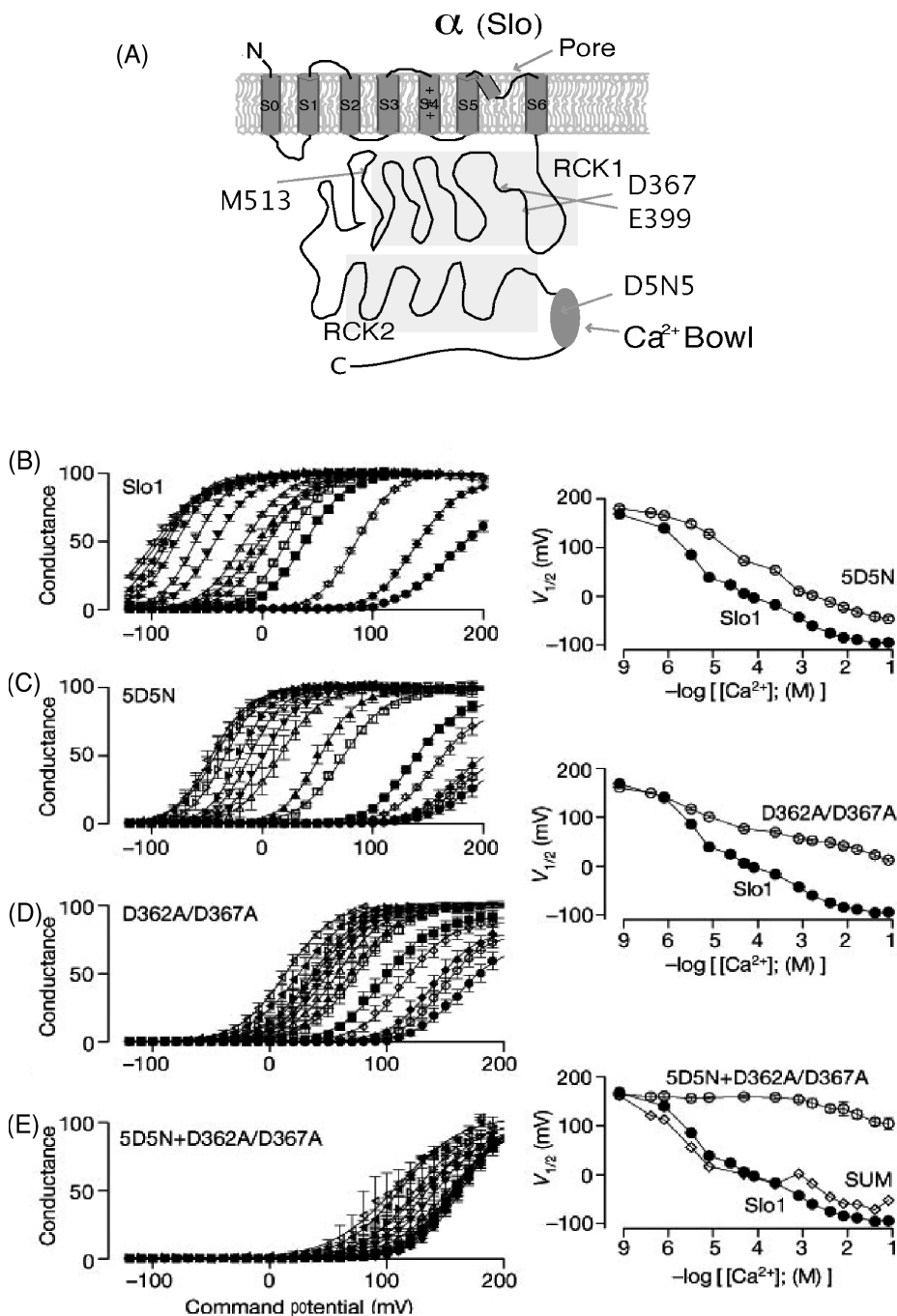
**Au: Please provide the missing characters.**

### 5.10 The BK<sub>Ca</sub> Channel Has Low-Affinity $\text{Ca}^{2+}$ Binding Sites

What is wrong with the HA model? It has yet to be compared quantitatively to single-channel data, and if it were to be, it is unlikely that it would reproduce the rapid flickers observed in such recordings (McManus and Magleby, 1988; Cox et al., 1997b; Rothberg and Magleby, 1999, 2000). Its fits to macroscopic-current kinetics in the middle  $[\text{Ca}^{2+}]$  range ( $\sim 10 \mu\text{M}$ ) could be improved, but the major problem with this model is that—like the VD-MWC model—it saturates at 100  $\mu\text{M}$   $[\text{Ca}^{2+}]$ , and therefore it does not predict additional  $G-V$  shifts at  $[\text{Ca}^{2+}]$  greater than this. This drawback was acknowledged by Horri gan and Aldrich and attributed to the lack in the model of the low-affinity  $\text{Ca}^{2+}$ -binding sites described by the Cui and Lingle groups (Shi and Cui, 2001; Zhang et al., 2001; Shi et al., 2002; Xia et al., 2002).

These binding sites were discovered by studying the effects of  $\text{Mg}^{2+}$  on BK<sub>Ca</sub>-channel gating. Both groups found that raising intracellular  $\text{Mg}^{2+}$  from 0 to 100 mM shifts the mSlo1  $G-V$  curve leftward  $\sim 100 \text{ mV}$ , and that this occurs in the presence or absence of 100–300  $\mu\text{M}$   $\text{Ca}^{2+}$ , as if  $\text{Mg}^{2+}$  were acting at separate sites from the  $\text{Ca}^{2+}$  binding sites. Furthermore, high  $\text{Mg}^{2+}$  prevents  $\text{Ca}^{2+}$  from causing leftward  $G-V$  shifts at concentrations greater than 100  $\mu\text{M}$ , and the mutation E399N (indicated in Fig. 5.13A) eliminates responses to  $\text{Ca}^{2+}$  above 100  $\mu\text{M}$  and  $\text{Mg}^{2+}$  up to 10 mM.

Daniel H. Cox



## 5. BK<sub>Ca</sub>-Channel Structure and Function

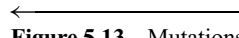
Thus, this mutation appears to eliminate a low-affinity Ca<sup>2+</sup>-binding site that is responsible for the leftward  $G-V$  shifts caused by [Ca<sup>2+</sup>] above 100 μM, and it is also the site of Mg<sup>2+</sup> action. Indeed when Zhang et al. (2001) added a low-affinity site to the 50-state model discussed above, they found that the model could produce leftward  $G-V$  shifts at high [Ca<sup>2+</sup>]. Thus, the BK<sub>Ca</sub> channel's ability to respond to [Ca<sup>2+</sup>] over five orders of magnitude is now understood to be due to the presence of both low- and high-affinity Ca<sup>2+</sup>-binding sites. The low-affinity site has been estimated to have the following dissociation constants for Ca<sup>2+</sup>:  $K_{C-Ca} 2-3$  mM (Zhang et al., 2001),  $K_{O-Ca} 0.6-0.9$  mM (Zhang et al., 2001), and for Mg<sup>2+</sup>:  $K_{C-Mg} 8-22$  mM (Shi and Cui, 2001; Zhang et al., 2001),  $K_{O-Mg} 2-6$  mM (Shi and Cui 2001; Zhang et al., 2001). Ca<sup>2+</sup>, therefore, binds weakly, but more tightly than Mg<sup>2+</sup>.

Under most physiological conditions, these low-affinity sites would not be occupied by Ca<sup>2+</sup>; however, as [Ca<sup>2+</sup>] rises transiently into the tens of micromolar—due to Ca<sup>2+</sup> entry through nearby Ca<sup>2+</sup> channels or release from intracellular stores—Ca<sup>2+</sup> binding at these sites may have a small effect (~10 mV  $G-V$  shift). Similarly, cytoplasmic [Mg<sup>2+</sup>] has been estimated to be ~0.5 to 1 mM (Zhang et al., 2001), a concentration that by acting through these sites would also be expected to produce a small  $G-V$  shift (10–25 mV). As yet, however, what role these low-affinity sites play in the functioning of the BK<sub>Ca</sub> channel in its native settings has yet to be explored.

### 5.11 The BK<sub>Ca</sub> Channel Has Two Types of High-Affinity Ca<sup>2+</sup>-Binding Sites

Another important insight that came in a part from mutagenesis work is that, rather than having a single type of high-affinity Ca<sup>2+</sup>-binding site, as the HA and the VD-MWC models assume, the BK<sub>Ca</sub> channel appears to have two structurally distinct, and structurally novel types of high-affinity Ca<sup>2+</sup>-binding sites.

The great majority of Ca<sup>2+</sup>-binding proteins thus far discovered (over 300 and counting) contain Ca<sup>2+</sup>-binding sites of the EF-hand type—calmodulin, troponin C, and parvalbumin for example. In these sites the Ca<sup>2+</sup> ion is coordinated in a pentagonal-bipyramidal arrangement by oxygen atoms from side chains of amino

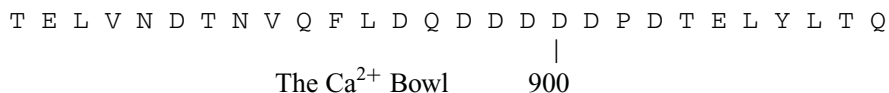
 **Figure 5.13** Mutations that affect BK<sub>Ca</sub>-channel Ca<sup>2+</sup> sensing. (A) Diagram of the Slo1 subunit indicating the putative RCK1 and RCK2 domains, the Ca<sup>2+</sup> bowl, and the positions of mutations D367A, E399A, M513I, and D5N5. (B) Wild-type mSlo1  $G-V$  curves plotted for the following [Ca<sup>2+</sup>] from right to left in μM: 0, 0.5, 1.4, 10.60, 100, 300, 1000, 2000, 5000, 10,000, 20,000, 50,000, 100,000. (C)  $G-V$  curves as in B for the Ca<sup>2+</sup>-bowl mutation 5D5N. (D)  $G-V$  curves as in B for the RCK1 mutation D362A/D367A. (E)  $G-V$  curves as in B for the double mutation 5D5N+D362A/D367A. On the right are shown  $V_{1/2}$  vs. [Ca<sup>2+</sup>] plots for the wildtype channel and the various mutations. Notice that the double mutation in E eliminates Ca<sup>2+</sup> sensing below 1 mM, and the sum of the  $V_{1/2}$  vs. [Ca<sup>2+</sup>] curves for the 5D5N mutation and the D362A/D367A mutation is very similar to the wild-type relation. This indicates that the two mutations are additive and likely acting on separate Ca<sup>2+</sup>-binding sites in Panels B–E are from figure 2 of Xia et al. (2002).

### Daniel H. Cox

acids spaced approximately every other residue over a loop of 12 residues (Falke et al., 1994). Typically EF-hands come in pairs with binding at one site allosterically affecting binding at the other site. Some proteins have as many as six EF hands, although two or four is more typical (Cox, 1996). The EF-hand consensus sequence is as follows: DX(D/N)X(D/N)-GX<sub>n</sub>DX<sub>n</sub>E (Falke et al., 1994). The BK<sub>Ca</sub> channel has no such sequence.

The other well established high-affinity Ca<sup>2+</sup>-binding motif is the C2 domain, which is found in such proteins as protein kinase C, phospholipase A2, and synaptotagmin. The C2 domain is composed of ~130 amino acids arranged in two four-stranded  $\beta$  sheets (Nalefski and Falke, 1996). Ca<sup>2+</sup> ions, usually two or three, are coordinated by acidic residues and backbone carbonyl groups in loops that lie above the  $\beta$ -stranded structure (Nalefski and Falke, 1996). The C2 domain also has a consensus sequence that does not conform to any region in the Slo1 subunit. What can be learned from these motifs, however, is that Ca<sup>2+</sup>-binding sites are likely to be found in loop regions containing acidic residues, often spaced every other residue.

Although Slo1 does not have any canonical Ca<sup>2+</sup>-binding motifs, there is a region in the distal portion of Slo1's C-terminal domain that roughly conforms to these criteria and has been strongly implicated as a Ca<sup>2+</sup> binding site. This region contains 28 amino acids, 10 of which are acidic.



It was given the name “the Ca<sup>2+</sup> bowl” (above) and proposed to be a Ca<sup>2+</sup>-binding site by Schreiber and Salkoff (1997) based on their observation that mutations in this region cause rightward  $G-V$  shifts at moderate and high [Ca<sup>2+</sup>], but no shift in the absence of Ca<sup>2+</sup> (Schreiber and Salkoff, 1997). Since then a number of observations have supported this conclusion. Principally, when a portion of Slo1 that includes the Ca<sup>2+</sup> bowl was transferred to the Ca<sup>2+</sup>-insensitive Slo3 subunit, Ca<sup>2+</sup>-sensitivity was conferred upon the previously insensitive channel (Schreiber et al., 1999). And peptides composed of portions of Slo1 that include the Ca<sup>2+</sup> bowl bind Ca<sup>2+</sup> in gel-overlay assays (Bian et al., 2001; Braun and Sy, 2001), and this binding is inhibited by the mutation of Ca<sup>2+</sup>-bowl aspartic acids (Bian et al., 2001; Bao et al., 2004).

Even large mutations in the Ca<sup>2+</sup> bowl, however, do not eliminate Ca<sup>2+</sup> sensing, but rather they reduce the  $G-V$  shift induced by 100  $\mu$ M Ca<sup>2+</sup> by about half (Xia et al., 2002). Where is the remaining Ca<sup>2+</sup> sensitivity coming from? One idea proposed by Schreiber and Salkoff (1997) is that in addition to the Ca<sup>2+</sup> bowl, the BK<sub>Ca</sub> channel has other high-affinity Ca<sup>2+</sup> binding sites. In support of this possibility they noted that Cd<sup>2+</sup> can activate the BK<sub>Ca</sub> channel, and that Ca<sup>2+</sup>-bowl mutations do not affect Cd<sup>2+</sup> sensing as they do Ca<sup>2+</sup> sensing. They proposed that Cd<sup>2+</sup> was binding selectively to a second high-affinity Ca<sup>2+</sup>-binding site that is unrelated to the Ca<sup>2+</sup> bowl.

## 5. BK<sub>Ca</sub>-Channel Structure and Function

Also supporting this hypothesis came work from the Moczydłowski, Cox, and Lingle groups who showed that large Ca<sup>2+</sup>-bowl mutants behave as if they have lost half of their high-affinity Ca<sup>2+</sup>-binding sites (Bian et al., 2001; Bao et al., 2002; Xia et al., 2002). And most importantly, mutations made far upstream of the Ca<sup>2+</sup> bowl in the proximal part of the intracellular domain, M513I (Bao et al., 2002) and D367A/D362A (Xia et al., 2002) (see Fig. 5.13A), also reduce the effectiveness of [Ca<sup>2+</sup>] in shifting the mSlo1 *G–V* relation (see Fig. 5.13B–D). And when either of these mutations is combined with a large Ca<sup>2+</sup>-bowl mutation, the channel's Ca<sup>2+</sup> sensitivity is either severely impaired (Bao et al., 2002) or eliminated up to 100 μM [Ca<sup>2+</sup>] (Fig. 5.13E). In fact, the Lingle group found that when they combined D367A/D362A with the Ca<sup>2+</sup>-bowl mutation D857-901N (5D5N) and the low-affinity-site mutation E399A, the channel's Ca<sup>2+</sup> response was completely eliminated up to 10 mM [Ca<sup>2+</sup>], and that D367A/D362A, unlike mutations made in the Ca<sup>2+</sup> bowl, also eliminated Cd<sup>2+</sup> sensing (Zeng et al., 2005)—consistent with the proposal that Cd<sup>2+</sup> binds only to the second site (Schreiber and Salkoff, 1997). Together, then, these results argue that the BK<sub>Ca</sub> channel has three types of Ca<sup>2+</sup>-binding sites, two of high affinity and one of low affinity, and the two of high affinity are thought to lie within different subdomains (proximal vs. distal) of the channel's large intracellular domain.

There is some disagreement as to the affinities of the two types of high-affinity sites. Bao et al. (2002) estimated the Ca<sup>2+</sup>-bowl-related site to have the following affinity constants for Ca<sup>2+</sup>:  $K_C = 3.5 \mu\text{M}$  and  $K_O = 0.8 \mu\text{M}$ , while Xia et al. (2002) made the following estimates  $K_C = 4.5 \mu\text{M}$  and  $K_O = 2.0 \mu\text{M}$ . For the other site Bao et al.'s estimates were  $K_C = 3.8 \mu\text{M}$  and  $K_O = 0.9 \mu\text{M}$ , similar to the Ca<sup>2+</sup>-bowl-related site, while the Xia et al.'s estimates (Bao et al., 2002) were considerably higher  $K_C = 17.2 \mu\text{M}$  and  $K_O = 4.6 \mu\text{M}$ . These groups, however, used different mutations and different models to make their estimates, so some disagreement is not surprising. Which are closer to the truth is as yet unclear.

When making the above estimates both groups relied on the assumption that there are four of each kind of binding site, one in each subunit. While this seems most reasonable, it is not necessarily the case. A lot depends on the symmetry of the intracellular portion of the channel and whether binding sites are contained within subunits or formed at their interfaces. If each type of binding site is contained within a subunit, and there are three types of binding sites, then the total is 12. If some of the binding sites are formed by the interfaces between subunits, and the cytoplasmic part of the channel is fourfold rotationally symmetric, then still there must be 12. But if the cytoplasmic part of the channel is twofold rotationally symmetric—a dimer of dimers, as is the case for the small conductance Ca<sup>2+</sup>-activated K<sup>+</sup> channel (Schumacher et al., 2001; Maylie et al., 2004)—then it could be that there are only two of each type of site. And indeed there could be combinations of sites, some at the interfaces and some within subunits, such that reasonably the channel could contain 6, 8, 10, or 12 Ca<sup>2+</sup> binding sites. Which is actually the case has yet to be definitively determined, however, it appears that there are four Ca<sup>2+</sup>-bowl-related sites, as when Niu and Magleby (2002) created hybrid channels that contained 1, 2,

### Daniel H. Cox

3, or 4 subunits mutated in the  $\text{Ca}^{2+}$  bowl, they observed four phenotypes. Indeed, this work also suggested that the binding of  $\text{Ca}^{2+}$  at one  $\text{Ca}^{2+}$ -bowl does not greatly affect binding at  $\text{Ca}^{2+}$  bowls on other subunits, something that was assumed without evidence in the modeling discussed above.

## 5.12 Is the $\text{BK}_{\text{Ca}}$ Channel Like the MthK Channel?

Another important question that has yet to be resolved is: how is the energy of  $\text{Ca}^{2+}$  binding transduced into energy for opening? This question may be difficult to answer without a crystal structure, but there is an interesting hypothesis from the bacterial world. In 2002, a crystal structure of MthK, a bacterial  $\text{Ca}^{2+}$ -activated  $\text{K}^+$  channel, was solved by the MacKinnon group (Jiang et al., 2002). Although this channel is very different from the  $\text{BK}_{\text{Ca}}$  channel in many respects—it contains only two membrane spanning helices and is not voltage-dependent—still it was proposed that the  $\text{BK}_{\text{Ca}}$  channel’s  $\text{Ca}^{2+}$  sensing mechanism may be much like that of the MthK channel (Jiang et al., 2001, 2002). The MthK channel is a fourfold symmetric tetramer with a classic  $\text{K}^+$ -channel pore sequence (TVGYG). Each monomer has an intracellular C-terminal domain whose core is an RCK domain (Jiang et al., 2001) (Fig. 5.14A). In the MthK structure eight RCK domains come together to form what is called the channel’s “gating ring” (Fig. 5.14B)—four from the channel proper and four more derived from a truncated piece of the channel generated off of a second translation start site. Each RCK domain in the gating ring binds one  $\text{Ca}^{2+}$ , and this—it has been proposed—causes a shearing motion that leads to an expansion of the ring and an opening of the channel’s gate (Jiang et al., 2002)(Fig. 5.14D).

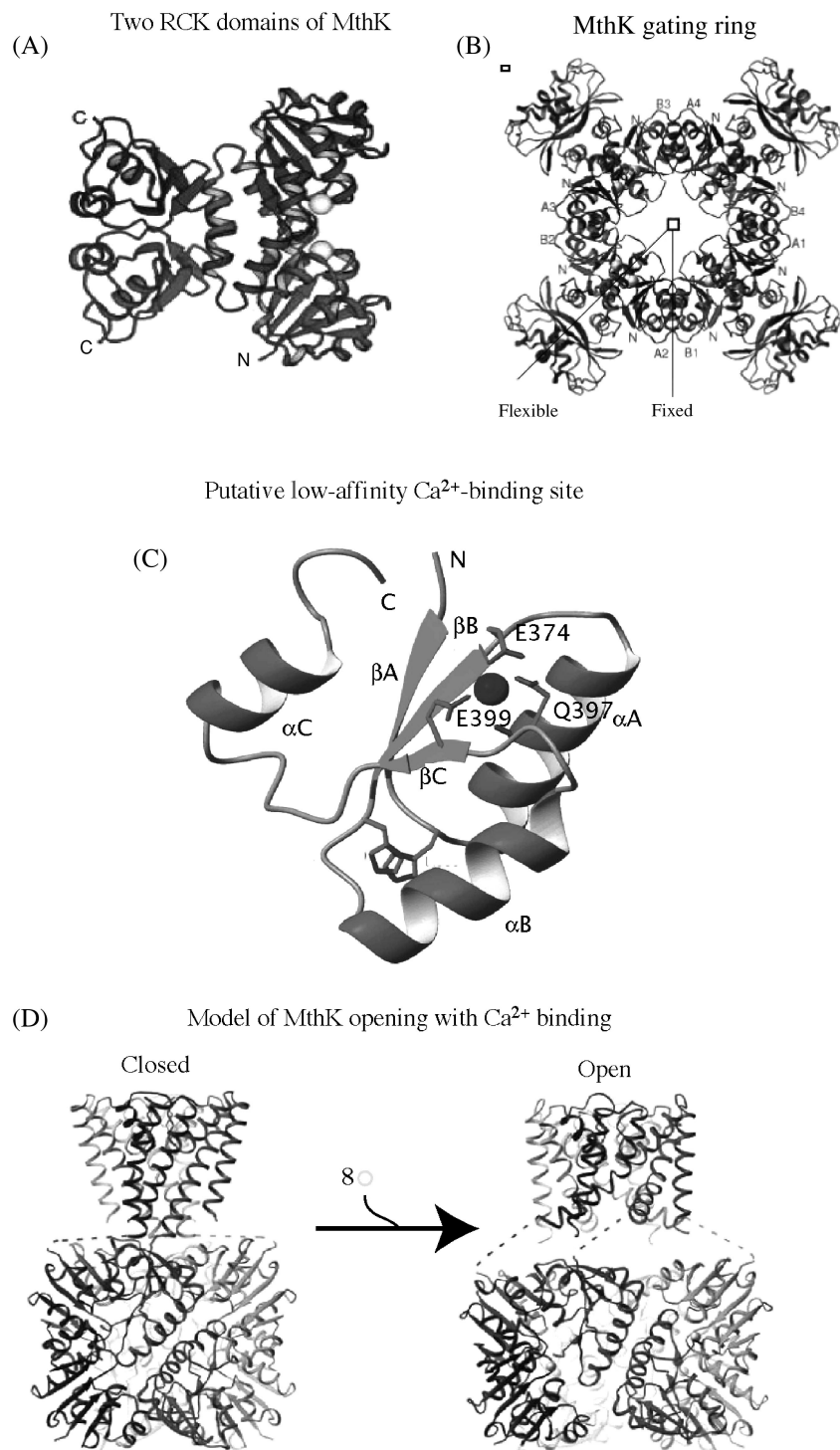
Even though the homology between proteins is low (<20%), because of key regions of conservation, and the mutagenesis experiments to be discussed below, the MacKinnon group has proposed that the Slo1 subunit has an RCK domain that forms the proximal part of its cytoplasmic domain (see Fig. 5.1B). Two lines of evidence support this proposition. First, in the crystal structure of an *E. coli* RCK domain—which takes the form of a Rossman fold—there is a salt bridge that is also predicted to exist in the putative RCK domain of Slo1. When Jiang et al. (2002) mutated the residues in the mSlo1 channel that are predicted to form this salt bridge

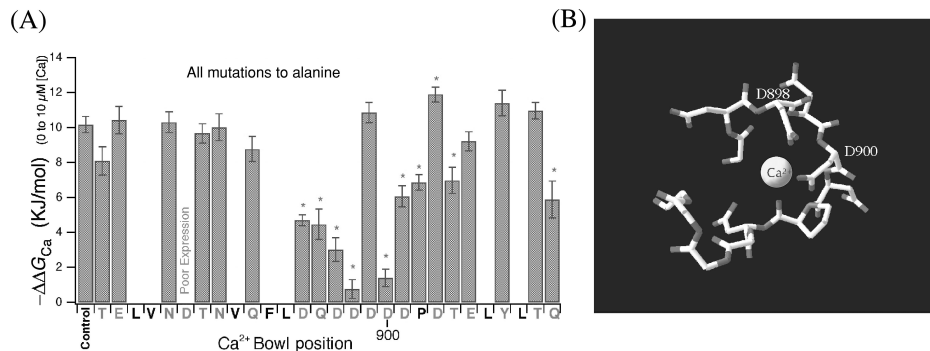
---

**Figure 5.14** The  $\text{Ca}^{2+}$ -sensing mechanism of the MthK channel. (A) Two RCK domains of the MthK channel. Spheres represent bound  $\text{Ca}^{2+}$  ions. (B) The “gating ring” of the MthK channel. This structure must be envisioned as hanging below the channel in the cytoplasm. It is composed of eight RCK domains. This crystal structure is from the work of Jiang et al. (2002). (C) Homology model of a portion of mSlo1 RCK1. Indicated are residues whose mutation disrupts low-affinity  $\text{Ca}^{2+}$  sensing and  $\text{Mg}^{2+}$  sensing. (□) Jiang et al. have proposed that as  $\text{Ca}^{2+}$  binds the gating ring expands, due to a rearrangement of its RCK domains, that leads to stress on the linkers leading to the pore helices, and this pulling action opens the channel. A, B, D were adapted from Jiang et al. (2002). C was adapted from Shi et al. (2002).

Au: Please provide the missing character.

## 5. BK<sub>Ca</sub>-Channel Structure and Function



**Daniel H. Cox**

**Figure 5.15** An alanine scan of the Ca<sup>2+</sup>-bowl. (A) On the horizontal axis are listed the residues of the Ca<sup>2+</sup> bowl. Each oxygen-containing side chain was mutated one at a time to alanine, and the resulting effect on the influence that 10 μM[Ca<sup>2+</sup>] has on the free energy difference between open and closed is plotted (Bao et al., 2004). These mutations were made in a M5I3I background to eliminate Ca<sup>2+</sup>-sensing through the RCK1-related high-affinity Ca<sup>2+</sup>-binding site (Bao et al., 2004). (B) Model from Bao et al. (2004) of Ca<sup>2+</sup> binding to the Ca<sup>2+</sup> bowl, based on the mutagenesis data in A. This figure was adapted from those in Bao et al. (2004).

to reverse their charges, if either residue were mutated alone, the channel's Ca<sup>2+</sup> sensitivity was reduced; however, if both residues were mutated together, near wild-type Ca<sup>2+</sup> sensitivity was restored. This result argues that a salt bridge was broken by each single mutation and then reformed by the double mutation, and therefore that the predicted salt bridge does exist in mSlo1. Second, the Cui group found that if they supposed that the RCK domain existed in Slo1 in the position predicted by Jiang et al., then mutations that they had identified as eliminating low-affinity Ca<sup>2+</sup> sensing, E399N and D374A, nicely clustered around a site where Ca<sup>2+</sup> or Mg<sup>2+</sup> could reasonably bind (Shi et al., 2002) (Fig. 5.14C). Thus, it seems likely that the proximal portion of Slo1's intracellular domain does form an RCK domain now referred to as RCK1.

The gating ring of the MthK channel is composed of eight RCK domains, while if each Slo1 subunit were to have one RCK domain, then that would make only four. The MacKinnon group however, has suggested that each Slo1 subunit has a second RCK domain downstream of the first, and, although they did not specify where it is, it is not difficult to identify a potential second RCK domain by homology to the first (Roosild et al., 2004). So perhaps there are two per subunit that come together to form an eight-membered gating ring like that of MthK. Indeed, consistent with this hypothesis Niu et al. (2004) found that the length of the linker between S6 and RCK1 has a large effect on the intrinsic energetics of channel opening. Lengthening the linker makes it harder to open the channel with depolarization, while shortening the linker makes it easier. Furthermore, lengthening the linker decreases the effectiveness of Ca<sup>2+</sup> at opening the channel. Although not the only plausible explanation, this is what might be expected if there is a gating ring that exerts an opening force on

## 5. BK<sub>Ca</sub>-Channel Structure and Function

the pore's S6 gate via these linkers, and this force increases as Ca<sup>2+</sup> binds and the gating ring expands.

Some data, however, suggest that the mechanism by which the BK<sub>Ca</sub> channel senses Ca<sup>2+</sup> must be different from that of the MthK channel. First, the acidic residues that bind Ca<sup>2+</sup> in MthK's RCK domain are not acidic in the Slo1 RCK domains. Second, the Slo1 residues M513 and D367 do not have counterparts in the MthK RCK domains. They lie in regions of sequence that are aligned as gaps with the MthK RCK sequence (Jiang et al., 2001, 2002). And third, the Ca<sup>2+</sup> bowl lies outside and downstream of both putative RCK domains of Slo1. Thus, the best candidates for Ca<sup>2+</sup>-binding sites in Slo1 do not exist in MthK, and the Ca<sup>2+</sup>-binding sites of MthK do not exist in Slo1. It could be, however, that the gating-ring structure is used by both channels, but the BK<sub>Ca</sub> channel has evolved a different mechanism for linking Ca<sup>2+</sup> binding sites to it.

One such binding site is apparently the Ca<sup>2+</sup> bowl, and it will be very interesting to see this domain's structure, as it is likely to reveal a novel Ca<sup>2+</sup>-binding site. Indeed, while no structure is yet available, Bao et al. (2004) mutated to alanine all of the oxygen containing side chains in the Ca<sup>2+</sup> bowl, and they determined that mutations at two positions eliminated Ca<sup>2+</sup> sensing via the Ca<sup>2+</sup>-bowl-related site, D898 and D900, while mutations at all other residues had less or no effect (Fig. 5.15A). They proposed that perhaps it is these residues and the backbone carbonyl oxygen of proline 902 that form the binding site (Fig. 5.15B). For now, however, this remains a working hypothesis.

### 5.13 The Discovery of β1

As discussed above, only a single BK<sub>Ca</sub>-channel gene has been identified (Pallanck and Ganetzky, 1994; Tseng-Crank et al., 1994; McCobb et al., 1995). Native BK<sub>Ca</sub> channels from various tissues, however, differ widely in their apparent Ca<sup>2+</sup> sensitivities (Latorre et al., 1989; McManus, 1991). In neurons and skeletal muscle, for example, the [Ca<sup>2+</sup>] at which BK<sub>Ca</sub> channels are half activated ([Ca]<sub>1/2</sub>) is between 5 and 100 μM at 0 mV, whereas in smooth muscle it is usually between 0.1 and 1 μM, and in some secretory cells it even lower (McManus, 1991). Some of this phenotypic diversity may arise from alternative RNA splicing, as nine splice sites and many alternative exons have been identified in mammalian slo1 sequences (Adelman et al., 1992; Butler et al., 1993; Pallanck and Ganetzky, 1994; Tseng-Crank et al., 1994; Ferrer et al., 1996; Saito et al., 1997; Xie and McCobb, 1998; Hanaoka et al., 1999; Langer et al., 2003). However, it now appears that the most important source of functional diversity is the regulated expression of BK<sub>Ca</sub>β subunits (Lu et al., 2006).

Although four α subunits form a functional channel, when Slo1 was purified from airway smooth muscle it was found to be associated with a smaller auxiliary subunit now termed β1 (Garcia-Calvo et al., 1994; Knaus et al., 1994a,b). When β1 was expressed with α, it was found to cause large leftward shifts in the channel's

### Daniel H. Cox

$G-V$  relation (Fig. 5.16A and B) such that at almost all voltages the channel becomes more  $\text{Ca}^{2+}$  sensitive (McManus et al., 1995). At 0 mV, for example, the  $\beta 1$  subunit enhances the apparent  $\text{Ca}^{2+}$  affinity of the mSlo channel by 10-fold (Bao and Cox, 2005) (Fig. 5.16C).  $\beta 1$  also generally slows macroscopic relaxation kinetics, particularly at hyperpolarized potentials (Dworetzky et al., 1996; Tseng-Crank et al., 1996) (Fig. 5.16D), it prolongs single-channel burst durations (Nimigean et al., 1999a,b), and it enhances the affinity of the channel for charybdotoxin (Hanner et al., 1997).

A question of recent interest has been how, in terms of the HA model, does the  $\beta 1$  subunit enhance the channel's  $\text{Ca}^{2+}$  sensitivity. While there is some controversy in this area (Bao and Cox, 2005; Oria and Latorre, 2005), three observations appear central. (1)  $\beta 1$  increases single-channel burst times even in the absence of  $\text{Ca}^{2+}$ , which indicates that  $\beta 1$  must be working, at least in part, on aspects of gating not involving  $\text{Ca}^{2+}$  binding (Nimigean et al., 1999b; Nimigean and Magleby, 2000); (2)  $\beta 1$  does not change the critical  $[\text{Ca}^{2+}]$  at which the  $\text{BK}_{\text{Ca}}$  channel's  $G-V$  relation starts to shift leftward  $\sim 100 \text{ nM}$  (Fig. 5.16E), which suggests that  $\beta 1$  does not greatly alter the affinity of the channel for  $[\text{Ca}^{2+}]$  when it is open  $K_C$  (Cox and Aldrich, 2000); and (3) gating current measurements reveal that  $\beta 1$  shifts the closed channel's  $Q_{\text{fast}}-V$  relation leftward along the voltage axis 71 mV (Bao and Cox 2005) (Fig. 5.16F). This makes the channel's voltage sensors activate at lower voltages, an effect that lowers the free energy difference between open and closed at most voltages, and thereby lowers the apparent affinity of the channel for  $\text{Ca}^{2+}$  as well. Indeed, by analyzing mSlo1 gating and ionic currents in terms an HA-like model with eight rather than four  $\text{Ca}^{2+}$  binding sites, Bao and Cox (2005), have suggested that  $\beta 1$ 's steady-state effects are due to a -71 mV shift in  $V_{hc}$ , a -61 mV shift in  $V_{ho}$ , and an increase in  $K_C$  from 3.7  $\mu\text{M}$  to 4.7  $\mu\text{M}$ . Thus, counter to what one might suppose, the  $\beta 1$  subunit enhances the  $\text{Ca}^{2+}$  sensitivity of the  $\text{BK}_{\text{Ca}}$  channel by apparently making the channel bind  $\text{Ca}^{2+}$  with lower affinity when it is closed, and making its voltage-sensors activate more easily.

## 5.14 Four $\beta$ Subunits Have Now Been Identified

Since the identification of  $\beta 1$ , three  $\beta 1$  homologues have been identified  $\beta 2-\beta 4$ . Their sequences are aligned with  $\beta 1$  in Fig. 5.17. Each has a unique tissue distribution and unique effects on channel gating.  $\beta 1$  is primarily found in smooth muscle (Tseng-Crank et al., 1996; Chang et al., 1997; Jiang et al., 1999), and  $\beta 1$ 's ability to enhance the  $\text{BK}_{\text{Ca}}$  channel's  $\text{Ca}^{2+}$  sensitivity has been shown to be critical for the proper regulation of smooth muscle tone (Brenner et al., 2000a).

$\beta 2$  is expressed at high levels in kidney, pancreas, ovary, and adrenal gland, at moderate levels in heart and brain, and at low levels in a wide variety of tissues (Wallner et al., 1999; Xia et al., 1999; Behrens et al., 2000; Uebel et al., 2000; Brenner et al., 2006). It has effects similar to  $\beta 1$  but it also has a longer N-terminus

## 5. BK<sub>Ca</sub>-Channel Structure and Function

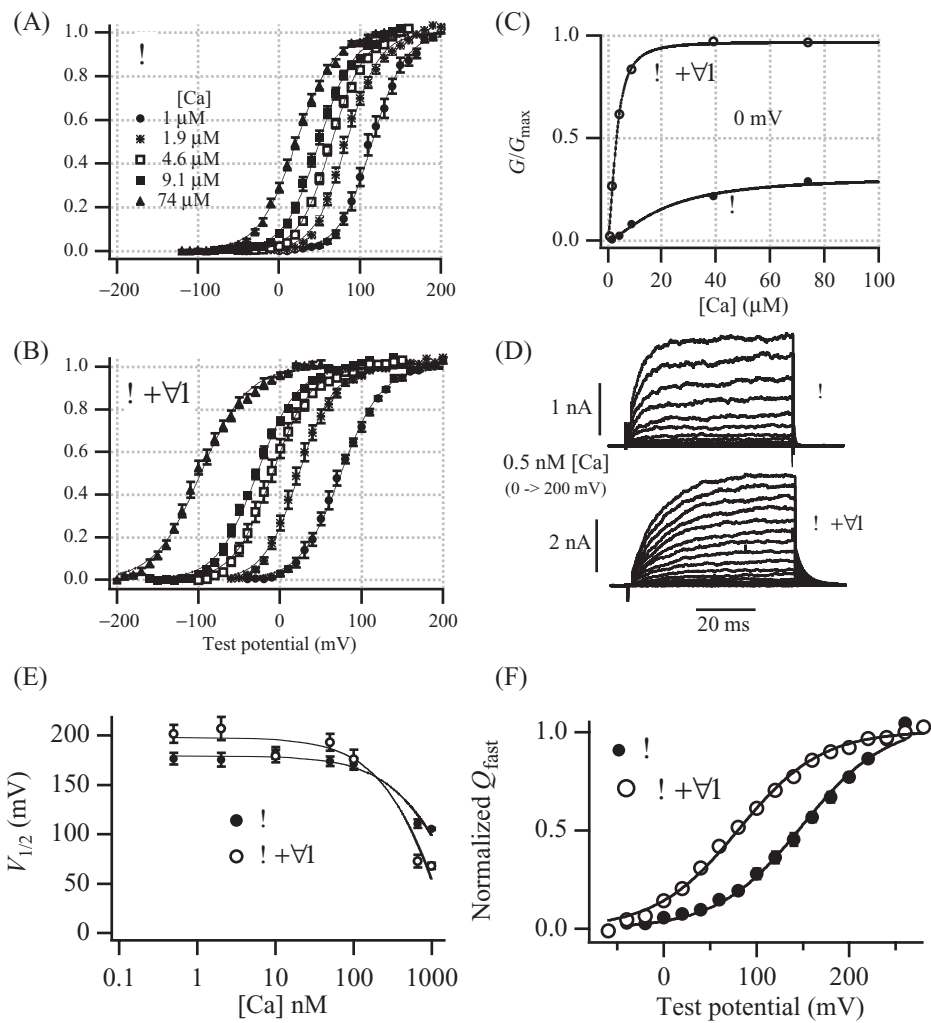


**Figure 5.16**  $\beta 1$  effects on BK<sub>Ca</sub>-channel gating.  $G-V$  relations determined from excised membrane patches expressing (A) the mSlo1<sub>α</sub> channel ( $\alpha$  subunit alone), or (B) mSlo1+ $\beta 1$  (bovine). (C) Ca<sup>2+</sup>-dose response curves for mSlo1<sub>α</sub> and mSlo1<sub>α+β1</sub>.  $[Ca^{2+}]_{1/2}$  for mSlo1<sub>α</sub> = 32.8  $\mu M$ ;  $[Ca^{2+}]_{1/2}$  for mSlo1<sub>α+β1</sub> = 3.4  $\mu M$  at 0 mV. (D) Macroscopic currents recorded from *Xenopus* oocyte macropatches expressing either mSlo1<sub>α</sub> or mSlo<sub>α+β1</sub>. Test potentials were between 0 and 200 mV.  $[Ca^{2+}]$  = 0.5 nM. Repolarizations were to -80 mV.  $V_{hold}$  = -50 mV. (E) Plots of  $V_{1/2}$  vs.  $[Ca^{2+}]$  for the mSlo1<sub>α</sub> and mSlo1<sub>α+β1</sub> channels. Notice both channels start to respond to  $[Ca^{2+}]$  at  $\sim 100$  nM. (F)  $Q_{fast}$  vs. voltage curves for the mSlo1 channel with and without  $\beta 1$ . Notice  $\beta 1$  shifts this relation 71 mV leftward without changing its slope. Panel E was adapted from Cox and Aldrich (2000). Panel F was adapted from Bao and Cox (2005).

Daniel H. Cox

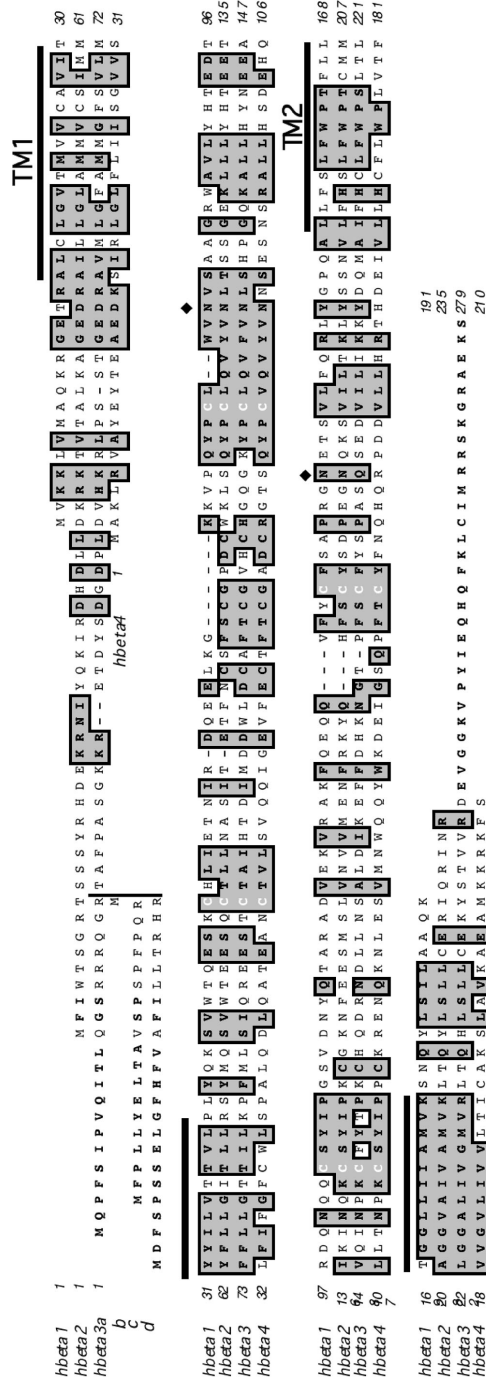


**Figure 5.17** Sequence alignment of human  $\beta$ 1 through  $\beta$ 4. The N-terminal alternative splice versions of  $\beta$ 3 are also shown. Transmembrane regions are overlined with dark bars. Conserved cysteines are indicated in white. N-linked glycosylation sites are indicated with  $\blacklozenge$ . Regions of sequence similarity are boxed and shaded.

## 5. BK<sub>Ca</sub>-Channel Structure and Function

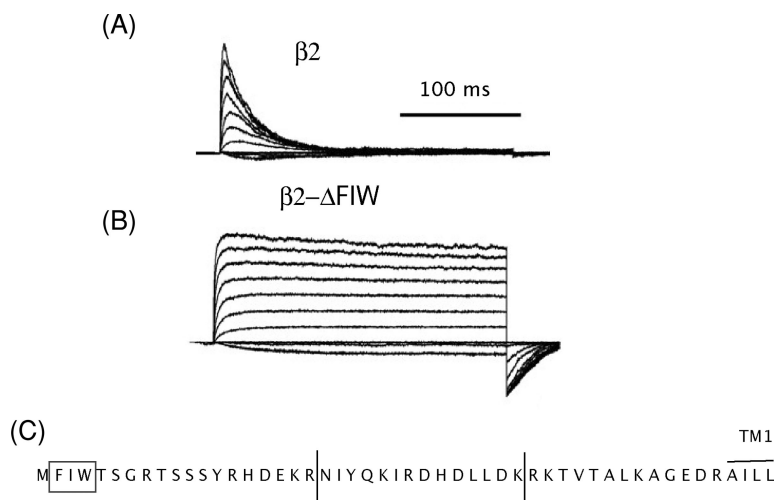


**Figure 5.18** The BK<sub>Ca</sub> β2 subunit caused an N-type inactivation. (A and B) Current family elicited with voltage steps from  $-100$  mV to  $+140$  mV from mSlo1 + β2 channels. Inactivation occurs with a time constant of 20–35 ms. (B) When the N-terminal residues FIW are deleted inactivation no longer occurs. (C) Sequence of the β2 N-terminus. Boxed are the residues deleted in B. Panels A and B were adapted from Xia et al. (2003).

that causes rapid N-type inactivation (Wallner et al., 1999; Xia et al., 1999, 2003; Brenner et al., 2000b) (Fig. 5.18A). Indeed, when the N-terminus of β2 is removed, inactivation is eliminated (Wallner et al., 1999; Xia et al., 1999), and when it is added back as a free peptide, inactivation is again observed as the peptide binds after the channel opens (Wallner et al., 1999). Thus, a “ball and chain” mechanism does seem to apply (Aldrich, 2001). Furthermore, Xia et al. (2003) found that residues 2–4 (FIW) are important determinants of inactivation rate and extent (Fig. 5.18B), while the nature of the residues between this sequence and the first transmembrane domain are not critical, so long as there are at least 12 of them. The β2 subunit is thought to underlie the inactivation of the BK<sub>Ca</sub> channels of adrenal chromaffin cells (Wallner et al., 1999; Xia et al., 1999).

β3 is expressed at low levels in a wide variety of tissues as well at high levels in testis, pancreas, and heart (Behrens et al., 2000; Brenner et al., 2000b; Uebele et al., 2000). It carries an unusually long C-terminus, and four splice variants of β3 (a–d) have been identified (Uebele et al., 2000) that differ from one another at their N-termini (see Fig. 5.17). β3a–c cause rapid inactivation that is mediated in each case by the subunit’s N-terminus (Uebele et al., 2000). The inactivation mediated by β3a and β3c is less complete than that mediated by β2 (Uebele et al., 2000), while β3b causes a very rapid inactivation (Xia et al., 2000; Uebele et al., 2000), so fast that it can only be observed as a decay in current at high voltages where activation is also very fast. β3d has no obvious effects on BK<sub>Ca</sub>-channel activation or inactivation; however, all β3 subunits cause a pronounced inward rectification that is mediated

### Daniel H. Cox

by the  $\beta 3$  extracellular loop (Zeng et al., 2003). This loop, it has been proposed, reaches over the top of the channel to interact with ions as they pass through the channel and toxins as they block the channel. Supporting this proposal,  $\alpha + \beta 3$  single-channel recordings show a rapid, flickery gating pattern that is removed when the cysteine residues of the external loop are reduced, and the disulfide bridges they form disrupted (Zeng et al., 2003).

The  $\beta 4$  subunit is found almost exclusively in the brain (Behrens et al., 2000; Brenner et al., 2000b; Weiger et al., 2000), and its main effect on the channel is to slow its kinetics (Behrens et al., 2000; Brenner et al., 2000b; Weiger et al., 2000; Ha et al., 2004). It also has small effects (compared to  $\beta 1$ ) on steady-state gating causing rightward  $G-V$  shifts at low  $[Ca^{2+}]$  and leftward  $G-V$  shifts at high  $[Ca^{2+}]$  (Behrens et al., 2000; Brenner et al., 2000b; Weiger et al., 2000; Ha et al., 2004).  $\beta 4$  knockout mice display prolonged action potentials in the dentate gyrus and seizures focused in this area (Brenner et al., 2005). The  $\beta 4$  subunit also renders the  $BK_{Ca}$  channel insensitive to block by charybdotoxin (Meera et al., 2000). There is still a great deal to be learned about how  $BK_{Ca}$   $\beta$  subunits produce their varied effects.

## 5.15 Conclusions

Over the last two decades a great deal has been learned about the genetics and biophysics of the  $BK_{Ca}$  channel. The *Slo1* gene was cloned. Sophisticated gating models have been produced.  $\beta$  subunits have been identified as an important source of functional diversity, and some progress has been made in the characterization of the channel's  $Ca^{2+}$ -sensing mechanism. In the coming decade the challenge will be to determine the structure of this channel and how this structure leads to the behaviors that have been so carefully documented and explained in energetic terms.

## References

- Adelman, J.P. et al. 1992. Calcium-activated potassium channels expressed from cloned complementary DNAs. *Neuron* 9:209–216.
- Aggarwal, S.K., and R. MacKinnon. 1996. Contribution of the S4 segment to gating charge in the Shaker  $K^+$  channel. *Neuron* 16:1169–1177.
- Aldrich, R.W. 2001. Fifty years of inactivation. *Nature* 411:643–644.
- Atkinson, N.S., G.A. Robertson, and B. Ganetzky. 1991. A component of calcium-activated potassium channels encoded by the *Drosophila slo* locus. *Science* 253:551–555.
- Bao, L., and D.H. Cox. 2005. Gating and ionic currents reveal how the  $BK_{Ca}$  channel's  $Ca^{2+}$  sensitivity is enhanced by its beta1 subunit. *J. Gen. Physiol.* 126:393–412.
- Bao, L., C. Kaldany, E.C. Holmstrand, and D.H. Cox. 2004. Mapping the  $BK_{Ca}$  channel's “ $Ca^{2+}$  bowl”: Side-chains essential for  $Ca^{2+}$  sensing. *J. Gen. Physiol.* 123:475–489.

## 5. BK<sub>Ca</sub>-Channel Structure and Function

- Bao, L., A.M. Rapin, E.C. Holmstrand, and D.H. Cox. 2002. Elimination of the BK(Ca) channel's high-affinity Ca(2+) sensitivity. *J. Gen. Physiol.* 120:173–189.
- Behrens, R. et al. 2000. hKCNMB3 and hKCNMB4, cloning and characterization of two members of the large-conductance calcium-activated potassium channel beta subunit family. *FEBS Lett.* 474:99–106.
- Bezanilla, F. 2005. Voltage-gated ion channels. *IEEE Trans. Nanobiosci.* 4:34–48.
- Bhattacharjee, A. et al. 2003. Slick (Slo2.1), a rapidly-gating sodium-activated potassium channel inhibited by ATP. *J. Neurosci.* 23:11681–11691.
- Bian, S., I. Favre, and E. Moczydlowski. 2001. Ca<sup>2+</sup>-binding activity of a COOH-terminal fragment of the Drosophila BK channel involved in Ca<sup>2+</sup>-dependent activation. *Proc. Natl. Acad. Sci. USA* 98:4776–4781.
- Blatz, A.L., and K.L. Magleby. 1984. Ion conductance and selectivity of single calcium-activated potassium channels in cultured rat muscle. *J. Gen. Physiol.* 84:1–23.
- Braun, A.F., and L. Sy. 2001. Contribution of potential EF hand motifs to the calcium-dependent gating of a mouse brain large conductance, calcium-sensitive K(+) channel. *J. Physiol.* 533:681–695.
- Brelidze, T.I., and K.L. Magleby. 2005. Probing the geometry of the inner vestibule of BK channels with sugars. *J. Gen. Physiol.* 126:105–121.
- Brelidze, T.I., X. Niu, and K.L. Magleby. 2003. A ring of eight conserved negatively charged amino acids doubles the conductance of BK channels and prevents inward rectification. *Proc. Natl. Acad. Sci. USA*.
- Brenner, R. et al. 2000. Vasoregulation by the  $\beta 1$  subunit of the calcium-activated potassium channel. *Nature* 407:870–876.
- Brenner, R., T.J. Jegla, A. Wickenden, Y. Liu, and R.W. Aldrich. 2000b. Cloning and functional characterization of novel large conductance calcium-activated potassium channel beta subunits, hKCNMB3 and hKCNMB4. *J. Biol. Chem.* 275:6453–6461.
- Brenner, R. et al. 2005. BK channel beta4 subunit reduces dentate gyrus excitability and protects against temporal lobe seizures. *Nat. Neurosci.*
- Butler, A., S. Tsunoda, D.P. McCobb, A. Wei, and L. Salkoff. 1993. mSlo, a complex mouse gene encoding “maxi” calcium-activated potassium channels. *Science* 261:221–224.
- Chang, C.P., S.I. Dworetzky, J. Wang, and M.E. Goldstein. 1997. Differential expression of the alpha and beta subunits of the large-conductance calcium-activated potassium channel: Implication for channel diversity. *Brain Res. Mol. Brain Res.* 45:33–40.
- Cox, D.H., and R.W. Aldrich. 2000. Role of the beta1 subunit in large-conductance Ca(2+)-activated K(+) channel gating energetics. Mechanisms of enhanced Ca(2+) sensitivity. *J. Gen. Physiol.* 116:411–432.
- Cox, D.H., J. Cui, and R.W. Aldrich. 1997. Separation of gating properties from permeation and block in mslo large conductance Ca-activated K<sup>+</sup> channels. *J. Gen. Physiol.* 109:633–646.

**Au:** Pls. provide the vol. number and page number for Brenner et al.

**Au:** Pls.  
provide the  
chapter title of  
the book in  
Cox (1996)

### Daniel H. Cox

- Cox, D.H., J. Cui, and R.W. Aldrich. 1997. Allosteric gating of a large conductance Ca-activated K<sup>+</sup> channel. *J. Gen. Physiol.* 110:257–281.
- Cox, J.A. 1996. In: Guidebook to the Calcium-Binding Proteins. M.R. Celio and T.L. Pauls, editors. Oxford University Press, Oxford, pp.1–14.
- Cui, J., and R.W. Aldrich. 2000. Allosteric linkage between voltage and Ca(2+)-dependent activation of BK-type mslo1 K(+) channels. *Biochemistry* 39:15612–15619.
- Cui, J., D.H. Cox, and R.W. Aldrich. 1997. Intrinsic voltage dependence and Ca<sup>2+</sup> regulation of mslo large conductance Ca-activated K<sup>+</sup> channels. *J. Gen. Physiol.* 109:647–673.
- DiChiara, T.J., and P.H. Reinhart. 1995. Distinct effects of Ca<sup>2+</sup> and voltage on the activation and deactivation of cloned Ca<sup>2+</sup>-activated K<sup>+</sup> channels. *J. Physiol. (Lond.)* 489:403–418.
- Diaz, L. et al. 1998. Role of the S4 segment in a voltage-dependent calcium-sensitive potassium (hSlo) channel. *J. Biol. Chem.* 273:32430–32436.
- Doyle, D.A. et al. 1998. The structure of the potassium channel: Molecular basis of K<sup>+</sup> conduction and selectivity. *Science* 280:69–77.
- Dworetzky, S.I. et al. 1996. Phenotypic alteration of a human BK (hSlo) channel by hSlobeta subunit coexpression: Changes in blocker sensitivity, activation/relaxation and inactivation kinetics, and protein kinase A modulation. *J. Neurosci.* 16:4543–4550.
- Falke, J.J., S.K. Drake, A.L. Hazard, and O.B. Peersen. 1994. Molecular tuning of ion binding to calcium signaling proteins. *Q. Rev. Biophys.* 27:219–290.
- Ferrer, M., M. Meyer, and G. Osol. 1996. Estrogen replacement increases beta-adrenoceptor-mediated relaxation of rat mesenteric arteries. *J. Vasc. Res.* 33:124–131.
- Garcia-Calvo, M. et al. 1994. Purification and reconstitution of the high-conductance, calcium-activated potassium channel from tracheal smooth muscle. *J. Biol. Chem.* 269:676–682.
- Goldstein, S.A., and C.A. Miller. 1992. A point mutation in a Shaker K<sup>+</sup> channel changes its charybdotoxin binding site from low to high affinity. *Biophys. J.* 62:5–7.
- Golowasch, J., A. Kirkwood, and C. Miller. 1986. Allosteric effects of Mg<sup>2+</sup> on the gating of Ca<sup>2+</sup>-activated K<sup>+</sup> channels from mammalian skeletal muscle. *J. Exp. Biol.* 124:5–13.
- Grissmer, S. et al. 1994. Pharmacological characterization of five cloned voltage-gated K<sup>+</sup> channels, types Kv1.1, 1.2, 1.3, 1.5, and 3.1, stably expressed in mammalian cell lines. *Mol. Pharmacol.* 45:1227–1234.
- Ha, T.S., M.S. Heo, and C.S. Park. 2004. Functional effects of auxiliary beta4-subunit on rat large-conductance Ca(2+)-activated K(+) channel. *Biophys. J.* 86:2871–2882.
- Hanaoka, K., J.M. Wright, I.B. Cheglakov, T. Morita, and W.B. Guggino. 1999. A 59 amino acid insertion increases Ca(2+) sensitivity of rbslo1, a Ca<sup>2+</sup> -activated K(+) channel in renal epithelia. *J. Membr. Biol.* 172:193–201.

## 5. BK<sub>Ca</sub>-Channel Structure and Function

- Hanner, M. et al. 1997. The beta subunit of the high-conductance calcium-activated potassium channel contributes to the high-affinity receptor for charybdotoxin. *Proc. Natl. Acad. Sci. USA* 94:2853–2858.
- Hanner, M. et al. 1998. The beta subunit of the high conductance calcium-activated potassium channel. Identification of residues involved in charybdotoxin binding. *J. Biol. Chem.* 273:16289–16296.
- Heginbotham, L., T. Abramson, and R. MacKinnon. 1992. A functional connection between the pores of distantly related ion channels as revealed by mutant K<sup>+</sup> channels. *Science* 258:1152–1155.
- Heginbotham, L., and R. MacKinnon. 1993. Conduction properties of the cloned Shaker K<sup>+</sup> channel. *Biophys. J.* 65:2089–2096.
- Hille, B. 1992. Ionic Channels of Excitable Membranes. Sinauer Associates, Sunderland, MA.
- Horrigan, F. T., and R.W. Aldrich. 1999. Allosteric voltage gating of potassium channels II. Mslo channel gating charge movement in the absence of Ca(2+). *J. Gen. Physiol.* 114:305–336.
- Horrigan, F.T., and R.W. Aldrich. 2002. Coupling between voltage sensor activation, Ca<sup>2+</sup> binding and channel opening in large conductance (BK) potassium channels. *J. Gen. Physiol.* 120:267–305.
- Horrigan, F.T., J. Cui, and R.W. Aldrich. 1999. Allosteric voltage gating of potassium channels I. Mslo ionic currents in the absence of Ca(2+). *J. Gen. Physiol.* 114:277–304.
- Jiang, Y., A. Pico, M. Cadene, B.T. Chait, and R. MacKinnon. 2001. Structure of the RCK domain from the *E. coli* K<sup>+</sup> channel and demonstration of its presence in the human BK channel. *Neuron* 29:593–601.
- Jiang, Y. et al. 2002. Crystal structure and mechanism of a calcium-gated potassium channel. *Nature* 417:515–522.
- Jiang, Y. et al. 2003. X-ray structure of a voltage-dependent K<sup>+</sup> channel. *Nature* 423:33–41.
- Jiang, Z., M. Wallner, P. Meera, and L. Toro. 1999. Human and rodent MaxiK channel beta-subunit genes: Cloning and characterization. *Genomics* 55:57–67.
- Knaus, H.G. et al. 1994. Primary sequence and immunological characterization of beta-subunit of high conductance Ca(2+)-activated K<sup>+</sup> channel from smooth muscle. *J. Biol. Chem.* 269:17274–17278.
- Knaus, H.G., M. Garcia-Calvo, G.J. Kaczorowski, and M.L. Garcia. 1994. Subunit composition of the high conductance calcium-activated potassium channel from smooth muscle, a representative of the mSlo and slowpoke family of potassium channels. *J. Biol. Chem.* 269:3921–3924.
- Kuo, A. et al. 2003. Crystal structure of the potassium channel KirBac1.1 in the closed state. *Science* 300:1922–1926.
- Langer, P., S. Grunder, and A. Rusch. 2003. Expression of Ca<sup>2+</sup>-activated BK channel mRNA and its splice variants in the rat cochlea. *J. Comp. Neurol.* 455:198–209.
- Latorre, R., A. Oberhauser, P. Labarca, and O. Alvarez. 1989. Varieties of calcium-activated potassium channels. *Annu. Rev. Physiol.* 51:385–399.

**Daniel H. Cox**

- Li, W., and R.W. Aldrich. 2004. Unique inner pore properties of BK channels revealed by quaternary ammonium block. *J. Gen. Physiol.* 124:43–57.
- Long, S.B., E.B. Campbell, and R. Mackinnon. 2005. Crystal structure of a mammalian voltage-dependent Shaker family K<sup>+</sup> channel. *Science* 309:897–903.
- Lu, R. et al. 2006. MaxiK channel partners: Physiological impact. *J. Physiol.* 570:65–72.
- MacKinnon, R. 2003. Potassium channels. *FEBS Lett.* 555:62–65.
- MacKinnon, R., L. Heginbotham, and T. Abramson. 1990. Mapping the receptor site for charybdotoxin, a pore-blocking potassium channel inhibitor. *Neuron* 5:767–771.
- MacKinnon, R., and C. Miller. 1998. Mechanism of charybdotoxin block of the high-conductance, Ca<sup>2+</sup>-activated K<sup>+</sup> channel. *J. Gen. Physiol.* 91:335–349.
- Magleby, K.L., and B.S. Pallotta. 1983. Burst kinetics of single calcium-activated potassium channels in cultured rat muscle. *J. Physiol. (Lond.)* 344:605–623.
- Markwardt, F., and G. Isenberg. 1992. Gating of maxi K<sup>+</sup> channels studied by Ca<sup>2+</sup> concentration jumps in excised inside-out multi-channel patches (myocytes from guinea pig urinary bladder). *J. Gen. Physiol.* 99:841–862.
- Maylie, J., C.T. Bond, P.S. Herson, W.S. Lee, and J.P. Adelman. 2004. Small conductance Ca<sup>2+</sup>-activated K<sup>+</sup> channels and calmodulin. *J. Physiol.* 554:255–261.
- McCobb, D.P. et al. 1995. A human calcium-activated potassium channel gene expressed in vascular smooth muscle. *Am. J. Physiol.* 269:H767–H777.
- McManus, O.B. 1991. Calcium-activated potassium channels: Regulation by calcium. *J. Bioenerg. Biomembr.* 23:537–560.
- McManus, O.B., and K.L. Magleby. 1988. Kinetic states and modes of single large-conductance calcium-activated potassium channels in cultured rat skeletal muscle. *J. Physiol. (Lond.)* 402:79–120.
- McManus, O.B., and K.L. Magleby. 1989. Kinetic time constants independent of previous single-channel activity suggest Markov gating for a large conductance Ca-activated K channel. *J. Gen. Physiol.* 94:1037–1070.
- McManus, O.B., and K.L. Magleby. 1991. Accounting for the Ca(2+)-dependent kinetics of single large-conductance Ca(2+)-activated K<sup>+</sup> channels in rat skeletal muscle. *J. Physiol. (Lond.)* 443:739–777.
- McManus, O.B. et al. 1995. Functional role of the beta subunit of high conductance calcium-activated potassium channels. *Neuron* 14:645–650.
- Meera, P., M. Wallner, Z. Jiang, and L. Toro. 1996. A calcium switch for the functional coupling between alpha (hslo) and beta subunits (KV,Ca beta) of maxi K channels. *FEBS Lett.* 382:84–88.
- Meera, P., M. Wallner, M. Song, and L. Toro. 1997. Large conductance voltage- and calcium-dependent K<sup>+</sup> channel, a distinct member of voltage-dependent ion channels with seven N-terminal transmembrane segments (S0–S6), an extracellular N terminus, and an intracellular (S9–S10) C terminus. *Proc. Natl. Acad. Sci. USA* 94:14066–14071.
- Meera, P., M. Wallner, and L.A. Toro. 2000. neuronal beta subunit (KCNMB4) makes the large conductance, voltage- and Ca<sup>2+</sup>-activated K<sup>+</sup> channel resistant

## 5. BK<sub>Ca</sub>-Channel Structure and Function

- to charybdotoxin and iberiotoxin. *Proc. Natl. Acad. Sci. USA* 97:5562–5567.
- Methfessel, C., and G. Boheim. 1982. The gating of single calcium-dependent potassium channels is described by an activation/blockade mechanism. *Biophys. Struct. Mech.* 9:35–60.
- Moczydlowski, E., and R. Latorre. 1983. Gating kinetics of Ca<sup>2+</sup>-activated K<sup>+</sup> channels from rat muscle incorporated into planar lipid bilayers. Evidence for two voltage-dependent Ca<sup>2+</sup> binding reactions. *J. Gen. Physiol.* 82:511–542.
- Monod, J., J. Wyman, and J.P. Changeux. 1965. On the nature of allosteric transitions: A plausible model. *J. Mol. Biol.* 12:88–118.
- Moss, G.W., J. Marshall, M. Morabito, J.R. Howe, and E. Moczydlowski. 1996. An evolutionarily conserved binding site for serine proteinase inhibitors in large conductance calcium-activated potassium channels. *Biochemistry* 35:16024–16035.
- Munujos, P., H.G. Knaus, G.J. Kaczorowski, and M.L. Garcia. 1995. Cross-linking of charybdotoxin to high-conductance calcium-activated potassium channels: Identification of the covalently modified toxin residue. *Biochemistry* 34:10771–10776.
- Nalefski, E.A., and J.J. Falke. 1996. The C2 domain calcium-binding motif: Structural and functional diversity. *Protein Sci.* 5:2375–2390.
- Nimigean, C.M., J.S. Chappie, and C. Miller. 2003. Electrostatic tuning of ion conductance in potassium channels. *Biochemistry* 42:9263–9268.
- Nimigean, C.M., and K.L. Magleby. 1999. β Subunits increase the calcium sensitivity of mSlo by stabilizing bursting kinetics. *Biophys. J.* 76(2):A328.
- Nimigean, C.M., and K.L. Magleby. 1999. The beta subunit increases the Ca<sup>2+</sup> sensitivity of large conductance Ca<sup>2+</sup>-activated potassium channels by retaining the gating in the bursting states. *J. Gen. Physiol.* 113:425–440.
- Nimigean, C.M., and K.L. Magleby. 2000. Functional coupling of the beta(1) subunit to the large conductance Ca(2+)-activated K(+) channel in the absence of Ca(2+). Increased Ca(2+) sensitivity from a Ca(2+)-independent mechanism. *J. Gen. Physiol.* 115:719–736.
- Niu, X., and K.L. Magleby. 2002. Stepwise contribution of each subunit to the cooperative activation of BK channels by Ca<sup>2+</sup>. *Proc. Natl. Acad. Sci. USA* 99:11441–11446.
- Niu, X., X. Qian, and K.L. Magleby. 2004. Linker-gating ring complex as passive spring and Ca(2+)-dependent machine for a voltage- and Ca(2+)-activated potassium channel. *Neuron* 42:745–756.
- Oberhauser, A., O. Alvarez, and R. Latorre. 1988. Activation by divalent cations of a Ca<sup>2+</sup>-activated K<sup>+</sup> channel from skeletal muscle membrane. *J. Gen. Physiol.* 92:67–86.
- Orio, P., and R. Latorre. 2005. Differential effects of beta 1 and beta 2 subunits on BK channel activity. *J. Gen. Physiol.* 125:395–411.
- Orio, P., P. Rojas, G. Ferreira, and R. Latorre. 2002. New disguises for an old channel: MaxiK channel beta-subunits. *News Physiol. Sci.* 17:156–161.

**Daniel H. Cox**

- Pallanck, L., and B. Ganetzky. 1994. Cloning and characterization of human and mouse homologs of the *Drosophila* calcium-activated potassium channel gene, *slowpoke*. *Hum. Mol. Genet.* 3:1239–1243.
- Pallotta, B.S. 1983. Single channel recordings from calcium-activated potassium channels in cultured rat muscle. *Cell Calcium* 4:359–370.
- Roosild, T.P., K.T. Le, and S. Choe. 2004. Cytoplasmic gatekeepers of K<sup>+</sup>-channel flux: A structural perspective. *Trends Biochem. Sci.* 29:39–45.
- Rothberg, B.S., and K.L. Magleby. 1999. Gating kinetics of single large-conductance Ca<sup>2+</sup>-activated K<sup>+</sup> channels in high Ca<sup>2+</sup> suggest a two-tiered allosteric gating mechanism. *J. Gen. Physiol.* 114:93–124.
- Rothberg, B.S., and K.L. Magleby. 2000. Voltage and Ca<sup>2+</sup> activation of single large-conductance Ca<sup>2+</sup>-activated K<sup>+</sup> channels described by a two-tiered allosteric gating mechanism. *J. Gen. Physiol.* 116:75–99.
- Saito, M., C. Nelson, L. Salkoff, and C.J. Lingle. 1997. A cysteine-rich domain defined by a novel exon in a slo variant in rat adrenal chromaffin cells and PC12 cells. *J. Biol. Chem.* 272:11710–11717.
- Schreiber, M. et al. 1998. Slo3, a novel pH-sensitive K<sup>+</sup> channel from mammalian spermatocytes. *J. Biol. Chem.* 273:3509–3516.
- Schreiber, M. and L. Salkoff. 1997. A novel calcium-sensing domain in the BK channel. *Biophys. J.* 73:1355–1363.
- Schreiber, M., A. Yuan, and L. Salkoff. 1999. Transplantable sites confer calcium sensitivity to BK channels. *Nat. Neurosci.* 2:416–421.
- Schumacher, M.A., A.F. Rivard, H.P. Bachinger, and J.P. Adelman. 2001. Structure of the gating domain of a Ca<sup>2+</sup>-activated K<sup>+</sup> channel complexed with Ca<sup>2+</sup>/calmodulin. *Nature* 410:1120–1124.
- Segel, I. 1993. *H. Enzyme Kinetics: Behavior and Analysis of Rapid Equilibrium and Steady-State Enzyme Systems*. Wiley-Interscience, New York.
- Seoh, S., D. Sigg, D.M. Papazian, and F. Bezanilla. 1996. Voltgae-sensing residues in the S2 and S4 segments of the *shaker* K<sup>+</sup> channel. *Neuron* 16:1159–1167.
- Shen, K.Z. et al. 1994. Tetraethylammonium block of Slowpoke calcium-activated potassium channels expressed in Xenopus oocytes: Evidence for tetrameric channel formation. *Pflugers Arch.* 426:440–445.
- Shi, J., and J. Cui. 2001. Intracellular Mg(2+) enhances the function of BK-type Ca(2+)-activated K(+) channels. *J. Gen. Physiol.* 118:589–606.
- Shi, J. et al. 2002. Mechanism of magnesium activation of calcium-activated potassium channels. *Nature* 418:876–880.
- Stefani, E. et al. 1997. Voltage-controlled gating in a large conductance Ca<sup>2+</sup>-sensitive K<sup>+</sup> channel (hslo). *Proc. Natl. Acad. Sci. USA* 94:5427–5431.
- Stocker, M., and C. Miller. 1994. Electrostatic distance geometry in a K<sup>+</sup> channel vestibule. *Proc. Natl. Acad. Sci. USA* 91:9509–9513.
- Talukder, G., and R.W. Aldrich. 2000. Complex voltage-dependent behavior of single unliganded calcium-sensitive potassium channels. *Biophys. J.* 78:761–772.
- Tang, X.D. et al. 2003. Haem can bind to and inhibit mammalian calcium-dependent Slo1 BK channels. *Nature* 425:531–535.

## 5. BK<sub>Ca</sub>-Channel Structure and Function

- Tseng-Crank, J. et al. 1994. Cloning, expression, and distribution of functionally distinct Ca(2+)-activated K<sup>+</sup> channel isoforms from human brain. *Neuron* 13:1315–1330.
- Tseng-Crank, J. et al. 1996. Cloning, expression, and distribution of a Ca(2+)-activated K<sup>+</sup> channel beta-subunit from human brain. *Proc. Natl. Acad. Sci. USA* 93:9200–9205.
- Uebele, V.N. et al. 2000. Cloning and functional expression of two families of beta-subunits of the large conductance calcium-activated K<sup>+</sup> channel. *J. Biol. Chem.* 275:23211–23218.
- Wallner, M., P. Meera, and L. Toro. 1996. Determinant for beta-subunit regulation in high-conductance voltage-activated and Ca(2+)-sensitive K<sup>+</sup> channels: An additional transmembrane region at the N terminus. *Proc. Natl. Acad. Sci. USA* 93:14922–14927.
- Wallner, M., P. Meera, and L. Toro. 1999. Molecular basis of fast inactivation in voltage and Ca<sup>2+</sup>-activated K<sup>+</sup> channels: A transmembrane beta-subunit homolog. *Proc. Natl. Acad. Sci. USA* 96:4137–4142.
- Wang, Y.W., J.P. Ding, X.M. Xia, and C.J. Lingle. 2002. Consequences of the stoichiometry of Slo1 alpha and auxiliary beta subunits on functional properties of large-conductance Ca<sup>2+</sup>-activated K<sup>+</sup> channels. *J. Neurosci.* 22:1550–1561.
- Webster, S.M., D. Del Camino, J.P. Dekker, and G. Yellen. 2004. Intracellular gate opening in Shaker K<sup>+</sup> channels defined by high-affinity metal bridges. *Nature* 428:864–868.
- Weiger, T.M. et al. 2000. A novel nervous system beta subunit that downregulates human large conductance calcium-dependent potassium channels. *J. Neurosci.* 20:3563–3570.
- Xia, X.M., J.P. Ding, and C.J. Lingle. 1999. Molecular basis for the inactivation of Ca<sup>2+</sup>- and voltage-dependent BK channels in adrenal chromaffin cells and rat insulinoma tumor cells. *J. Neurosci.* 19:5255–5264.
- Xia, X.M., J.P. Ding, and C.J. Lingle. 2003. Inactivation of BK channels by the NH<sub>2</sub> terminus of the beta2 auxiliary subunit: An essential role of a terminal peptide segment of three hydrophobic residues. *J. Gen. Physiol.* 121:125–148.
- Xia, X.M., J.P. Ding, X.H. Zeng, K.L. Duan, and C.J. Lingle. 2000. Rectification and rapid activation at low Ca<sup>2+</sup> of Ca<sup>2+</sup>-activated, voltage-dependent BK currents: consequences of rapid inactivation by a novel beta subunit. *J. Neurosci.* 20:4890–4903.
- Xia, X.M., X. Zeng, and C.J. Lingle. 2002. Multiple regulatory sites in large-conductance calcium-activated potassium channels. *Nature* 418:880–884.
- Xie, J., and D.P. McCobb. 1998. Control of alternative splicing of potassium channels by stress hormones. *Science* 280:443–446.
- Yellen, G. 1984. Ionic permeation and blockade in Ca<sup>2+</sup>-activated K<sup>+</sup> channels of bovine chromaffin cells. *J. Gen. Physiol.* 84:157–186.
- Yuan, A. et al. 2000. SLO-2, a K<sup>+</sup> channel with an unusual Cl<sup>-</sup> dependence. *Nat. Neurosci.* 3:771–779. taf/DynaPage.taf?file=/neuro/journal/v3/n8/full/nn0800\_771.html; taf/DynaPage.taf?file=/neuro/journal/v3/n8/abs/nn0800\_771.html.

**Daniel H. Cox**

- Zagotta, W.N., T. Hoshi, J. Dittman, and R.W. Aldrich. 1994. Shaker potassium channel gating. II: Transitions in the activation pathway. *J. Gen. Physiol.* 103:279–319.
- Zeng, X.H., X.M. Xia, and C.J. Lingle. 2003. Redox-sensitive extracellular gates formed by auxiliary beta subunits of calcium-activated potassium channels. *Nat. Struct. Biol.* 10:448–454.
- Zeng, X.H., X.M. Xia, and C.J. Lingle. 2005. Divalent cation sensitivity of BK channel activation supports the existence of three distinct binding sites. *J. Gen. Physiol.* 125:273–286.
- Zhang, X., C.R. Solaro, and C.J. Lingle. 2001. Allosteric regulation of BK channel gating by Ca(2+) and Mg(2+) through a nonselective, low affinity divalent cation site. *J. Gen. Physiol.* 118:607–636.